

CERN-PH-EP-2013-049

Submitted to: Phys. Rev. D

**Search for non-pointing photons in the diphoton and E_T^{miss}
final state in $\sqrt{s} = 7$ TeV proton–proton collisions
using the ATLAS detector**

The ATLAS Collaboration

Abstract

A search has been performed for photons originating in the decay of a neutral long-lived particle, exploiting the capabilities of the ATLAS electromagnetic calorimeter to make precise measurements of the flight direction of photons, as well as the calorimeter's excellent time resolution. The search has been made in the diphoton plus missing transverse energy final state, using the full data sample of 4.8 fb^{-1} of 7 TeV proton–proton collisions collected in 2011 with the ATLAS detector at the LHC. No excess is observed above the background expected from Standard Model processes. The results are used to set exclusion limits in the context of Gauge Mediated Supersymmetry Breaking models, with the lightest neutralino being the next-to-lightest supersymmetric particle and decaying with a lifetime in excess of 0.25 ns into a photon and a gravitino.

Search for non-pointing photons in the diphoton and E_T^{miss} final state in $\sqrt{s} = 7$ TeV proton–proton collisions using the ATLAS detector

The ATLAS Collaboration

A search has been performed for photons originating in the decay of a neutral long-lived particle, exploiting the capabilities of the ATLAS electromagnetic calorimeter to make precise measurements of the flight direction of photons, as well as the calorimeter’s excellent time resolution. The search has been made in the diphoton plus missing transverse energy final state, using the full data sample of 4.8 fb^{-1} of 7 TeV proton–proton collisions collected in 2011 with the ATLAS detector at the LHC. No excess is observed above the background expected from Standard Model processes. The results are used to set exclusion limits in the context of Gauge Mediated Supersymmetry Breaking models, with the lightest neutralino being the next-to-lightest supersymmetric particle and decaying with a lifetime in excess of 0.25 ns into a photon and a gravitino.

PACS numbers: 12.60.Jv, 13.85.Qk, 13.85.Rm

I. INTRODUCTION

Supersymmetry (SUSY) [1–9], a theoretically well-motivated candidate for physics beyond the Standard Model (SM), predicts the existence of a new SUSY partner (sparticle) for each of the SM particles, with identical quantum numbers except differing by half a unit of spin. In R-parity conserving SUSY models [10–14], these sparticles could be produced in pairs in proton–proton (pp) collisions at the CERN Large Hadron Collider (LHC), and would decay in cascades involving other sparticles and SM particles until the lightest SUSY particle (LSP), which is stable, is produced. In Gauge Mediated Supersymmetry Breaking (GMSB) models [15–20], the LSP is the gravitino (\tilde{G}). GMSB phenomenology is largely determined by the properties of the next-to-lightest supersymmetric particle (NLSP). The results of this analysis are presented in the context of the so-called Snowmass Points and Slopes parameter set 8 (SPS8) [21], which describes a set of minimal GMSB models with the lightest neutralino ($\tilde{\chi}_1^0$) as the NLSP. In the SPS8 set of models, the effective scale of SUSY breaking, denoted Λ , is a free parameter. In addition, the $\tilde{\chi}_1^0$ proper decay length, $c\tau(\tilde{\chi}_1^0)$, is a free parameter of the theory.

For the range of SPS8 Λ values relevant for this analysis, SUSY production is dominated by electroweak pair production of gauginos, and in particular of $\tilde{\chi}_2^0\tilde{\chi}_1^\pm$ and $\tilde{\chi}_1^+\tilde{\chi}_1^-$ pairs. In the SPS8 models, the dominant decay mode of the NLSP is $\tilde{\chi}_1^0 \rightarrow \gamma + \tilde{G}$. Previous ATLAS analyses have assumed prompt NLSP decays, with $c\tau(\tilde{\chi}_1^0) < 0.1$ mm, and therefore searched for an excess production of diphoton events that, due to the escaping gravitinos, exhibit significant missing transverse momentum (E_T^{miss}). The latest such ATLAS results [22] use the full 2011 dataset and, within the context of SPS8 models, exclude values of $\Lambda < 196$ TeV, corresponding to $m(\tilde{\chi}_1^0) > 280$ GeV, at the 95% confidence level (CL). The limits on SPS8 models are less stringent in the case of a longer-lived NLSP. For example, recent CMS 95% CL limits [23], obtained using the E_T^{miss} spectrum of events

with at least three jets and one or two photons, coupled with measurements of the photon arrival time, require $m(\tilde{\chi}_1^0) > 220$ GeV for $c\tau(\tilde{\chi}_1^0)$ values up to 500 mm.

The analysis reported in this paper uses the full data sample of 4.8 fb^{-1} of 7 TeV pp collisions collected in 2011 with the ATLAS detector at the LHC, and considers the scenario where the $\tilde{\chi}_1^0$ has a finite lifetime and can travel some distance from its production point before decaying. The search is performed in an inclusive sample of candidate diphoton + E_T^{miss} events.

The long-lived NLSP scenario introduces the possibility of a decay photon being produced after a finite delay and with a flight direction that does not point back to the primary vertex (PV) of the event. The analysis searches for such “non-pointing photons” by exploiting the fine segmentation of the ATLAS electromagnetic (EM) calorimeter to measure the flight direction of photons. The variable used as a measure of the degree of non-pointing of the photon is z_{DCA} , the difference between the z -coordinate¹ of the photon extrapolated back to its distance-of-closest-approach (DCA) to the beamline (i.e. $x = y = 0$) and z_{PV} , the z -coordinate of the PV. The search for non-pointing photons is then performed by fitting the shape of the z_{DCA} distribution obtained for photons in the signal region, defined as diphoton events with $E_T^{\text{miss}} > 75$ GeV, to a combination of templates that describe the z_{DCA} distribution for the expected signal and background events. In addition, the excellent time resolution of the calorimeter is exploited to measure the arrival times of the photons, providing a cross-check of the results.

¹ ATLAS uses a right-handed coordinate system with its origin at the nominal interaction point (IP) in the center of the detector and the z -axis along the beam pipe. The x -axis points from the IP to the center of the LHC ring, and the y -axis points upward. Cylindrical coordinates (r, ϕ) are used in the transverse plane, ϕ being the azimuthal angle around the beam pipe. The pseudorapidity is defined in terms of the polar angle θ as $\eta = -\ln \tan(\theta/2)$.

II. THE ATLAS DETECTOR

The ATLAS detector [24] covers nearly the entire solid angle around the collision point, and consists of an inner tracking detector surrounded by a solenoid, EM and hadronic calorimeters, and a muon spectrometer incorporating three large toroidal magnet systems. The ATLAS inner-detector system (ID) is immersed in a 2 T axial magnetic field, provided by a thin superconducting solenoid located before the calorimeters, and provides charged particle tracking in the pseudorapidity range $|\eta| < 2.5$. The ID consists of three detector subsystems, beginning closest to the beamline with the high-granularity silicon pixel detector, followed at larger radii by the silicon microstrip tracker and then the straw-tube-based transition radiation tracker. The ID allows an accurate reconstruction of tracks from the primary pp collision and precise determination of the location of the PV. The ID also identifies tracks from secondary vertices, permitting the efficient identification of photons that convert to electron-positron pairs as they pass through the detector material.

This analysis relies heavily on the capabilities of the ATLAS calorimeter system, which covers the pseudorapidity range $|\eta| < 4.9$. Finely-segmented EM calorimetry is provided by barrel ($|\eta| < 1.475$) and end-cap ($1.375 < |\eta| < 3.2$) lead/liquid-argon (lead/LAr) EM sampling calorimeters. An additional thin LAr presampler covering $|\eta| < 1.8$ allows corrections for energy losses in material upstream of the EM calorimeters. Hadronic calorimetry is provided by a steel/scintillator-tile calorimeter, segmented into three barrel structures within $|\eta| < 1.7$, and two copper/LAr hadronic end-cap calorimeters. The solid angle coverage is completed with forward copper/LAr and tungsten/LAr calorimeter modules optimized for EM and hadronic measurements, respectively. Outside the ATLAS calorimeters lies the muon spectrometer, which identifies and measures the deflection of muons up to $|\eta| = 2.7$, in a magnetic field generated by superconducting air-core toroidal magnet systems.

A. Pointing resolution

The EM calorimeter is segmented into three layers in depth, that are used to measure the longitudinal profile of the shower. The first layer uses highly granular “strips” segmented in the η direction, designed to allow efficient discrimination between single photon showers and two overlapping showers originating, for example, from the decay of a π^0 meson. The second layer collects most of the energy deposited in the calorimeter by EM showers initiated by electrons or photons. Very high energy showers can leave significant energy deposits in the third layer, which can also be used to correct for energy leakage beyond the EM calorimeter. By measuring precisely the centroids of the EM shower in the first and second

layers, the flight direction of photons can be determined. In the ATLAS $H \rightarrow \gamma\gamma$ analysis [25] that contributed to the discovery of a Higgs-like particle, this capability of the EM calorimeter was used to help choose the PV from which the two photons originated, thereby improving the diphoton invariant mass resolution and sensitivity of the search. The analysis described in this paper uses the measurement of the photon flight direction to search for photons that do not point back to the PV. The angular resolution of the EM calorimeter’s measurement of the flight direction of prompt photons is about $60 \text{ mrad}/\sqrt{E}$, where E is the energy measured in GeV. This angular precision corresponds, in the EM barrel calorimeter, to a resolution on z_{DCA} of about 15 mm for prompt photons with energies in the range of 50–100 GeV. Given the geometry, the z_{DCA} resolution is worse for photons reconstructed in the end-cap calorimeters, so the pointing analysis is restricted to photon candidates in the EM barrel calorimeter.

While the geometry of the EM calorimeter has been optimized for detecting particles that point back to near the nominal interaction point at the center of the detector (i.e. $x = y = z = 0$), the fine segmentation allows good pointing performance to be achieved over a wide range of photon impact angles. Figure 1 shows, as a function of $|z_{\text{DCA}}|$, the expected pointing resolution for SPS8 signal photons from Monte Carlo (MC) simulations, obtained by fitting to a Gaussian the difference between the value of z_{DCA} obtained from the calorimeter measurement and the MC generator-level information. The pointing resolution degrades with increasing $|z_{\text{DCA}}|$, but remains much smaller than $|z_{\text{DCA}}|$ in the region where the signal is expected.

The calorimeter pointing performance has been verified in data by using the finite spread of the LHC collision region along the z -axis. Superimposed on Figure 1 is the pointing resolution achieved for a sample of electrons from $Z \rightarrow ee$ events, where the distance, z_{PV} , between the PV and the nominal center of the detector serves the role of z_{DCA} . In this case, the pointing resolution is obtained by fitting to a Gaussian the difference between z_{PV} , as determined with high precision using tracking information, and the calorimeter measurement of the origin of the electron, along the beamline. Figure 1 shows that similar pointing performance is observed for photons and for electrons, as expected given their similar EM shower developments. This similarity validates the use of a sample of electrons from $Z \rightarrow ee$ events to study the pointing performance for photons. The expected pointing performance for electrons in a MC sample of $Z \rightarrow ee$ events is also shown on Figure 1, and is consistent with the data. The level of agreement between MC simulation and data over the range of values that can be accessed in the data gives confidence in the extrapolation using MC simulation to the larger deviations from pointing characteristic of the signal photons.

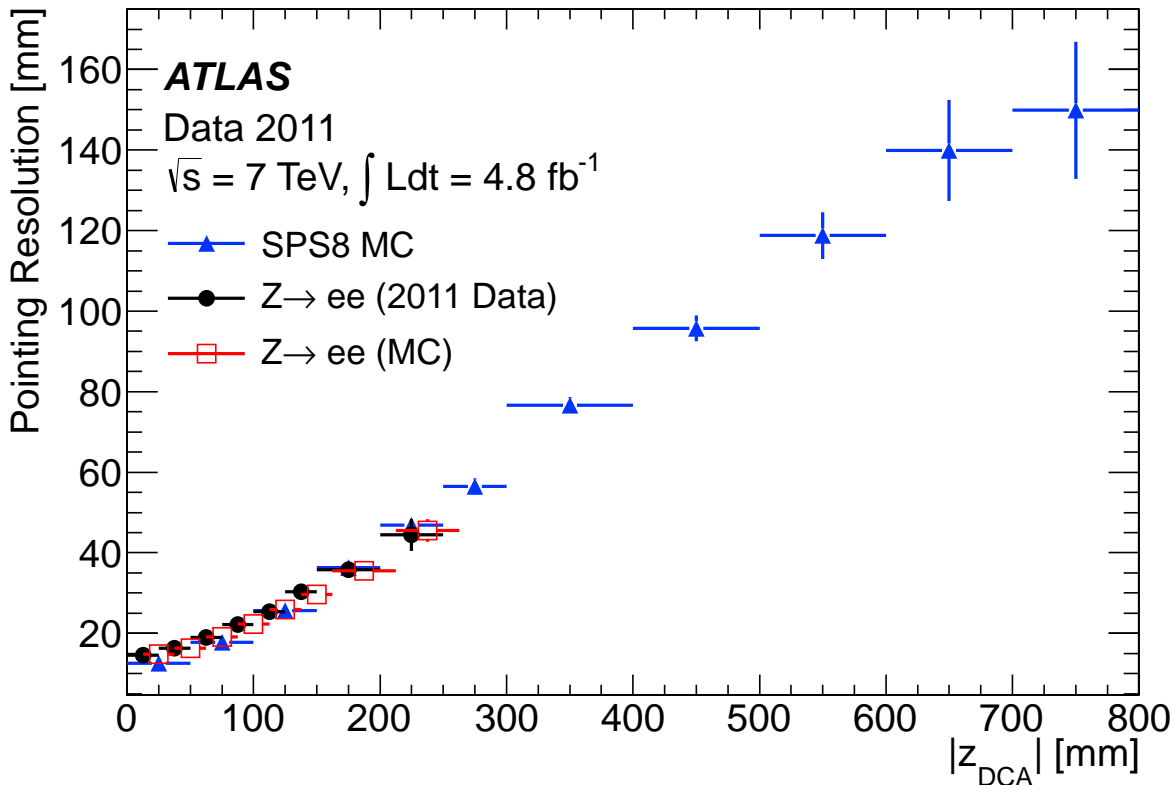


FIG. 1. Pointing resolution obtained for EM showers in the ATLAS LAr EM barrel calorimeter. The pointing resolution for photons from GMSB signal MC samples is plotted as a function of $|z_{\text{DCA}}|$. The pointing resolution is also shown for $Z \rightarrow ee$ data and MC, for which the primary vertex position, z_{PV} , serves the role of z_{DCA} .

B. Timing resolution

Photons from NLSP decays would reach the LAr calorimeter with a slight delay compared to prompt photons. This delay results mostly from the flight time of the heavy NLSP, as well as some effect due to the longer geometric path of a non-pointing photon produced in the NLSP decay. The EM calorimeter, with its novel “accordion” design, and its readout, which incorporates fast shaping, has excellent timing performance. Quality control tests during production of the electronics required the clock jitter on the LAr readout boards to be less than 20 ps, with typical values of 10 ps [26]. Calibration tests of the overall electronic readout performed *in situ* in the ATLAS cavern show a timing resolution of ≈ 70 ps [27], limited not by the readout but by the jitter of the calibration pulse injection system. Test-beam measurements [28] of production EM barrel calorimeter modules demonstrated a timing resolution of ≈ 100 ps in response to high energy electrons.

For this analysis, the arrival time of an EM shower is measured using the second-layer EM calorimeter cell with the maximum energy deposit. During 2011, the various LAr channels were timed-in online with a precision of about 1 ns. A large sample of $W \rightarrow e\nu$ events was used

to determine several calibration corrections which were applied to further optimize the timing resolution for EM clusters. The calibration includes corrections of various offsets in the timing of individual channels, corrections for the energy dependence of the timing, and flight-path corrections depending on the position of the PV. The corrections determined using the $W \rightarrow e\nu$ events were subsequently applied to electron candidates in $Z \rightarrow ee$ events to validate the procedure as well as to determine the timing performance in an independent data sample. Figure 2 shows the time resolution achieved as a function of the energy deposited in the second-layer cell used in the time measurement. The time resolution, $\sigma(t)$, is expected to follow the form $\sigma(t) = a/E \oplus b$, where E is the energy measured in GeV and \oplus indicates addition in quadrature. Superimposed on Figure 2 is the result of a fit of the resolution to this form, where the parameters a and b multiply the so-called noise term and constant term, respectively. A timing resolution of ≈ 290 ps is achieved for a large energy deposit. By comparing the arrival times of the two electrons in $Z \rightarrow ee$ events, this resolution is understood to include a correlated contribution of ≈ 220 ps, as expected due to the spread in pp collision times caused by the lengths of individual proton bunches along the LHC beamline. Subtracting this beam

contribution in quadrature, the obtained timing resolution for the calorimeter is ≈ 190 ps.

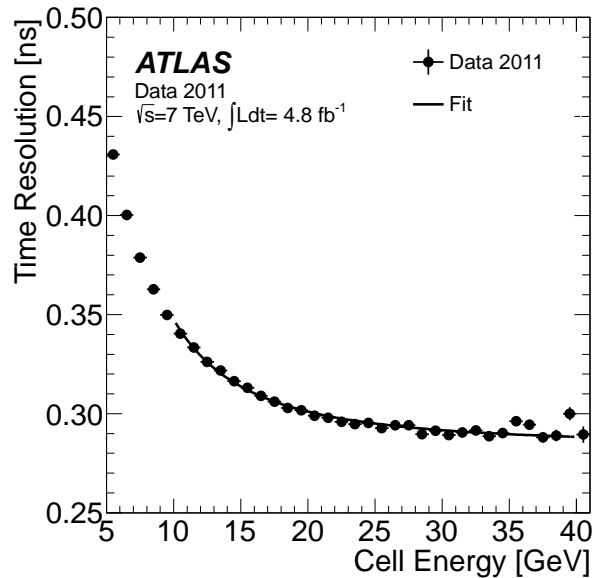


FIG. 2. Time resolution obtained for EM showers in the ATLAS LAr EM barrel calorimeter, as a function of the energy deposited in the second-layer cell with the maximum deposited energy. Superimposed is the result of the fit described in the text. The data are shown for electrons read out using high gain, and the errors shown are statistical only.

To cover the full dynamic range of physics signals of interest, the ATLAS LAr calorimeter readout boards [26] employ three overlapping linear gain scales, dubbed high, medium, and low, where the relative gain of successive scale is reduced by a factor of about ten. For a given event, any individual LAr readout channel is digitized using the gain scale that provides optimal energy resolution, given the energy deposited in that calorimeter cell. The results in Figure 2 are those obtained for electrons where the time was measured using a second-layer cell read out using high gain, for which the $W \rightarrow e\nu$ sample used to calibrate the timing is large. Calibration samples for the medium and low gain scales are smaller, resulting in reduced precision. The timing resolutions obtained are about 400 ps for medium gain and about 1 ns for low gain.

III. DATA AND MONTE CARLO SIMULATION SAMPLES

This analysis uses a data sample of pp collisions at a center-of-mass-energy of $\sqrt{s} = 7$ TeV, recorded with the ATLAS detector in 2011. The data sample, after applying quality criteria that require all ATLAS subdetector systems to be functioning normally, corresponds to a total integrated luminosity of $4.8 \pm 0.1 \text{ fb}^{-1}$.

While all background studies, apart from some cross-checks, are performed with data, MC simulations are used to study the response to SPS8 GMSB signal models, as a function of the free parameters Λ and $c\tau$. The other SPS8 model parameters are fixed to the following values: the messenger mass $M_{\text{mess}} = 2\Lambda$, the number of SU(5) messengers $N_5 = 1$, the ratio of the vacuum expectation values of the two Higgs doublets $\tan\beta = 15$, and the Higgs-sector mixing parameter $\mu > 0$ [21]. The SPS8 SUSY mass spectra, branching ratios and decay widths are calculated using ISAJET [29] version 7.80. The signal yield is normalized to the central value of the GMSB signal cross section, as calculated at next-to-leading order (NLO) using PROSPINO [30] version 2.1 with the CTEQ6.6m [31] parton distribution functions (PDFs). The total uncertainty on the signal cross section, times the signal acceptance and efficiency, from varying the PDFs and factorization and renormalization scales, as described in Ref. [32], ranges from 4.7% to 6.4%, depending on Λ .

The Herwig++ generator version 2.4.2 [33] with MRST 2007 LO* [34] PDFs is used to generate the signal MC samples. The branching ratio of the $\tilde{\chi}_1^0 \rightarrow \gamma + \tilde{G}$ decay mode is fixed to unity. Signal samples were generated for fixed values of Λ , ranging from 70 TeV to 210 TeV in 10 TeV steps, and for a variety of values of the NLSP lifetime. The performance for any lifetime can be obtained by reweighting as a function of lifetime the existing samples for a given value of Λ . The current analysis considers NLSP lifetime values in excess of 0.25 ns.

All MC samples were processed with the simulation [35] of the ATLAS detector based on GEANT4 [36] and were reconstructed with the same algorithms used for the data. The presence of additional pp interactions (pile-up) as a function of the instantaneous luminosity is taken into account by overlaying simulated minimum bias events according to the distribution of the number of pile-up interactions observed in data, with an average of about nine interactions per bunch crossing. The MC samples were generated with a spatial distribution of the PV consistent with that observed in the data. The simulated LAr time values are smeared such that the time resolution matches the performance, as described in Sec. II B, observed in data.

IV. OBJECT RECONSTRUCTION AND IDENTIFICATION

The reconstruction of converted and unconverted photons and of electrons is described in Refs. [37] and [38], respectively. Shape variables computed from the lateral and longitudinal energy profiles of the EM shower in the calorimeter are used to identify photons and discriminate against backgrounds. Two sets of selection criteria, denoted “loose” and “tight”, are defined [37]. The loose photon identification, designed for high photon efficiency with modest background rejection, uses variables

describing the shower shape in the second layer of the EM calorimeter, as well as leakage of energy into the hadronic calorimeter. The tight photon identification, designed for higher purity photon identification with still reasonable efficiency, includes more stringent cuts on these variables, as well as requirements on additional variables describing the shower in the first layer of the EM calorimeter. The various selection criteria do not depend on the transverse momentum of the photon (E_T), but do vary as a function of η in order to take into account variations in the calorimeter geometry and in the thickness of the upstream material. For more details, see Ref. [37].

The measurement of E_T^{miss} [39] is based on energy deposits in calorimeter cells inside three-dimensional clusters with $|\eta| < 4.5$. The energy of each cluster is calibrated to correct for the different response to electromagnetically and hadronically induced showers, energy loss in dead material, and out-of-cluster energy. The value of E_T^{miss} is corrected for contributions from any muons identified in the event, by adding in the energy derived from the properties of reconstructed muon tracks.

V. EVENT SELECTION

The selected events were collected by an online trigger requiring the presence of at least two loose photon candidates, each with $E_T > 20$ GeV and $|\eta| < 2.5$. To ensure the selected events resulted from a beam collision, events are required to have at least one PV candidate with five or more associated tracks. In case of multiple vertices, the PV is chosen as the vertex with the greatest sum of the square of the transverse momenta of all associated tracks.

The offline photon selection requires the two photon candidates to each have $E_T > 50$ GeV, and to satisfy $|\eta| < 2.37$, excluding the transition region of $1.37 < |\eta| < 1.52$ between the barrel and end-cap EM calorimeters. In addition, both photons are required to be isolated: after correcting for contributions from pile-up and the deposition ascribed to the photon itself [37], the transverse energy deposited in the calorimeter in a cone of $\Delta R = \sqrt{(\Delta\eta)^2 + (\Delta\phi)^2} = 0.2$ around each photon candidate must be less than 5 GeV [40].

Due mostly to the inclusion of cuts on the EM shower shape in the very finely segmented strips of the first EM calorimeter layer, the efficiency of the tight photon identification decreases with $|z_{\text{DCA}}|$ for values of $|z_{\text{DCA}}|$ larger than ≈ 100 mm. The loose efficiency remains flat over a wider range of $|z_{\text{DCA}}|$, up to values of ≈ 250 mm, after which it decreases less rapidly than the tight efficiency. The event selection requires at least one of the isolated photon candidates to pass the tight photon identification requirements, while the other must pass the loose photon identification cuts. The selected sample will therefore be referred to hereafter as the Tight–Loose (TL) diphoton sample. To reduce the potential bias in the pointing measurement that results from applying the photon identifi-

cation requirements, only the loose photon in each event is examined for evidence of non-pointing. The η cut on the loose photon is tightened to restrict it to lie in the EM barrel calorimeter, namely $|\eta| < 1.37$.

The TL diphoton sample is divided into exclusive sub-samples according to the value of E_T^{miss} . The TL sample with $E_T^{\text{miss}} < 20$ GeV is used, as described in Sec. VIB, to model the prompt backgrounds. The TL events with intermediate E_T^{miss} values, namely $20 \text{ GeV} < E_T^{\text{miss}} < 75$ GeV, are used as a control sample to validate the analysis procedure. The final signal region, which contains a total of 46 selected events, is defined by applying to the TL diphoton sample the additional requirement that the value of E_T^{miss} exceeds 75 GeV.

Table I summarizes the total acceptance times efficiency of the selection requirements, for examples of SPS8 signal model points with various values of Λ and τ . For fixed Λ , the acceptance falls approximately exponentially with increasing τ , dominated by the requirement that both NLSPs decay inside the ATLAS tracking detector (which extends to a radius of 107 cm) so that the decay photons are detected by the EM calorimeters. For fixed τ , the acceptance increases with increasing Λ , since the SUSY particle masses increase, leading the decay cascades to produce, on average, higher E_T^{miss} and also higher E_T values of the decay photons.

τ (ns)	Λ (TeV)		
	80	120	160
0.25	15.3 ± 0.3	29.6 ± 0.3	45.1 ± 0.3
1	11.1 ± 0.1	27.0 ± 0.2	35.9 ± 0.3
6	2.01 ± 0.02	5.38 ± 0.02	8.06 ± 0.06
20	0.39 ± 0.01	1.006 ± 0.005	1.43 ± 0.01
40	0.175 ± 0.005	0.384 ± 0.002	0.510 ± 0.004
80	0.090 ± 0.004	0.164 ± 0.001	0.196 ± 0.002

TABLE I. The total signal acceptance times efficiency, in percent, of the event selection requirements, for sample SPS8 model points with various Λ and τ values. The uncertainties shown are statistical only.

VI. SIGNAL AND BACKGROUND MODELING

A. SPS8 GMSB signal

The shape of the z_{DCA} distribution, alternately denoted hereafter as the pointing distribution, that is expected for photons from NLSP decays in events passing the selection cuts is determined using the SPS8 GMSB MC signal samples described previously, for various values of Λ and τ . The signal pointing distributions, normalized to unit area, are used as signal templates, hereafter referred to as T_{sig} . Since the T_{sig} shape is determined using MC simulations, systematic uncertainties in the

shape are included to account for possible differences in pointing performance between MC simulation and data. In particular, the presence of pile-up in the collisions could impact the pointing resolution, due both to energy deposits in the calorimeter from additional minimum bias collisions and to the possibility of misidentifying the PV. These effects are modeled in the MC simulation. However, as a conservative estimate of the systematic T_{sig} shape variations that could occur due to pile-up, the differences are taken between the nominal shape and those from the two subsamples which are obtained by dividing the MC samples roughly in two according to the number of PV candidates identified in each event. The T_{sig} distributions, along with their statistical and total uncertainties, are shown in Figure 3 for $\Lambda = 120$ TeV and for NLSP lifetime values of $\tau = 0.5$ and 30 ns.

B. Backgrounds

The background is expected to be completely dominated by pp collision events, with possible backgrounds due to cosmic rays, beam-halo events, or other non-collision processes being negligible. The source of the loose photon in background events contributing to the selected TL sample is expected to be either a prompt photon, an electron misidentified as a photon, or a jet misidentified as a photon. In each case, the object providing the loose photon signature originates from the PV. The pointing and timing distributions expected for these background sources are determined using data control samples.

Given their similar EM shower developments, the pointing resolution is similar for prompt photons and for electrons. The z_{DCA} distribution expected for prompt photons and for electrons is therefore modeled using electrons in $Z \rightarrow ee$ data events. The $Z \rightarrow ee$ event selection requires a pair of oppositely charged electron candidates, each of which has $p_{\text{T}} > 25$ GeV and $|\eta| < 2.37$ (excluding the transition region between the barrel and end-cap calorimeters). One of the electron candidates, dubbed the “tag”, is required to pass additional selection cuts on the EM shower topology and tracking information designed to identify a high-purity sample of electrons. The second electron candidate, dubbed the “probe”, is restricted to the range $|\eta| < 1.37$. The dielectron invariant mass is required to agree with the value of the Z mass within 10 GeV, a requirement that produces a sufficiently clean sample of $Z \rightarrow ee$ events. To avoid any bias, the pointing resolution for electrons is determined using the distribution measured for the probe electrons. The pointing distribution determined from $Z \rightarrow ee$ events, normalized to unit area, is used as the pointing template for prompt photons and electrons, and is referred to hereafter as $T_{e/\gamma}$.

While the EM showers of electrons and photons are similar, there are some differences. In particular, electrons traversing the material of the ID may

emit bremsstrahlung photons, widening the resulting EM shower. In addition, photons can convert into electron-positron pairs in the material of the ID. In general, the EM showers of unconverted photons are slightly narrower than those of electrons, which are in turn slightly narrower than those of converted photons. The EM component of the background in the signal region includes a mixture of electrons, converted photons, and unconverted photons. Therefore, using electrons from $Z \rightarrow ee$ events to model the EM showers of the loose photon candidates in the signal region can slightly underestimate the pointing resolution in some cases, and slightly overestimate it in others. The pointing distribution from $Z \rightarrow ee$ events is taken as the nominal $T_{e/\gamma}$ shape. The distributions from MC samples of unconverted and converted photons, with similar kinematic properties as expected for signal photons, are separately taken to provide conservative estimates of the possible variations in the $T_{e/\gamma}$ shape which could result from not separating these various contributions. The $T_{e/\gamma}$ distribution, along with its statistical and total uncertainties, is shown superimposed on Figure 3.

Due to their wider showers in the calorimeter, jets have a wider z_{DCA} distribution than prompt photons and electrons. The sample of events passing the TL selection, but with the additional requirement that $E_{\text{T}}^{\text{miss}} < 20$ GeV, is used as a data control sample that includes jets with properties similar to the background contributions expected in the signal region. The $E_{\text{T}}^{\text{miss}}$ requirement serves to render negligible any possible signal contribution in this control sample. The shape of the z_{DCA} distribution for the loose photon in these events, normalized to unit area, is used as a template, referred to hereafter as $T_{E_{\text{T}}^{\text{miss}} < 20 \text{ GeV}}$, in the final fit to the signal region. The TL sample with $E_{\text{T}}^{\text{miss}} < 20$ GeV should be dominated by jet-jet, jet- γ and $\gamma\gamma$ events. Therefore, the $T_{E_{\text{T}}^{\text{miss}} < 20 \text{ GeV}}$ template includes contributions from photons as well as from jets faking the loose photon signature. When using the template in the fit to extract the final results, it is not necessary to separate the photon and jet contributions. Instead, the relative fraction of the two background templates is treated as a nuisance parameter in the fitting procedure, as discussed in Sec. VIII.

The pointing resolution depends on the value of E_{T} of the photon candidate. Applying the shape of the $T_{E_{\text{T}}^{\text{miss}} < 20 \text{ GeV}}$ template to describe events in the signal region, defined with $E_{\text{T}}^{\text{miss}} > 75$ GeV, therefore implicitly relies on the assumption that the E_{T} distributions for photon candidates are similar in both regions. However, since $E_{\text{T}}^{\text{miss}}$ is essentially a negative vector sum of the E_{T} values of the energy depositions in the calorimeter, it is expected that there should be a correlation between the value of $E_{\text{T}}^{\text{miss}}$ and the E_{T} distributions of the physics objects in the event. This correlation is indeed observed in the TL control regions: the samples with higher $E_{\text{T}}^{\text{miss}}$ values have higher average photon E_{T} values. Increasing the minimum E_{T} requirement on the photons to

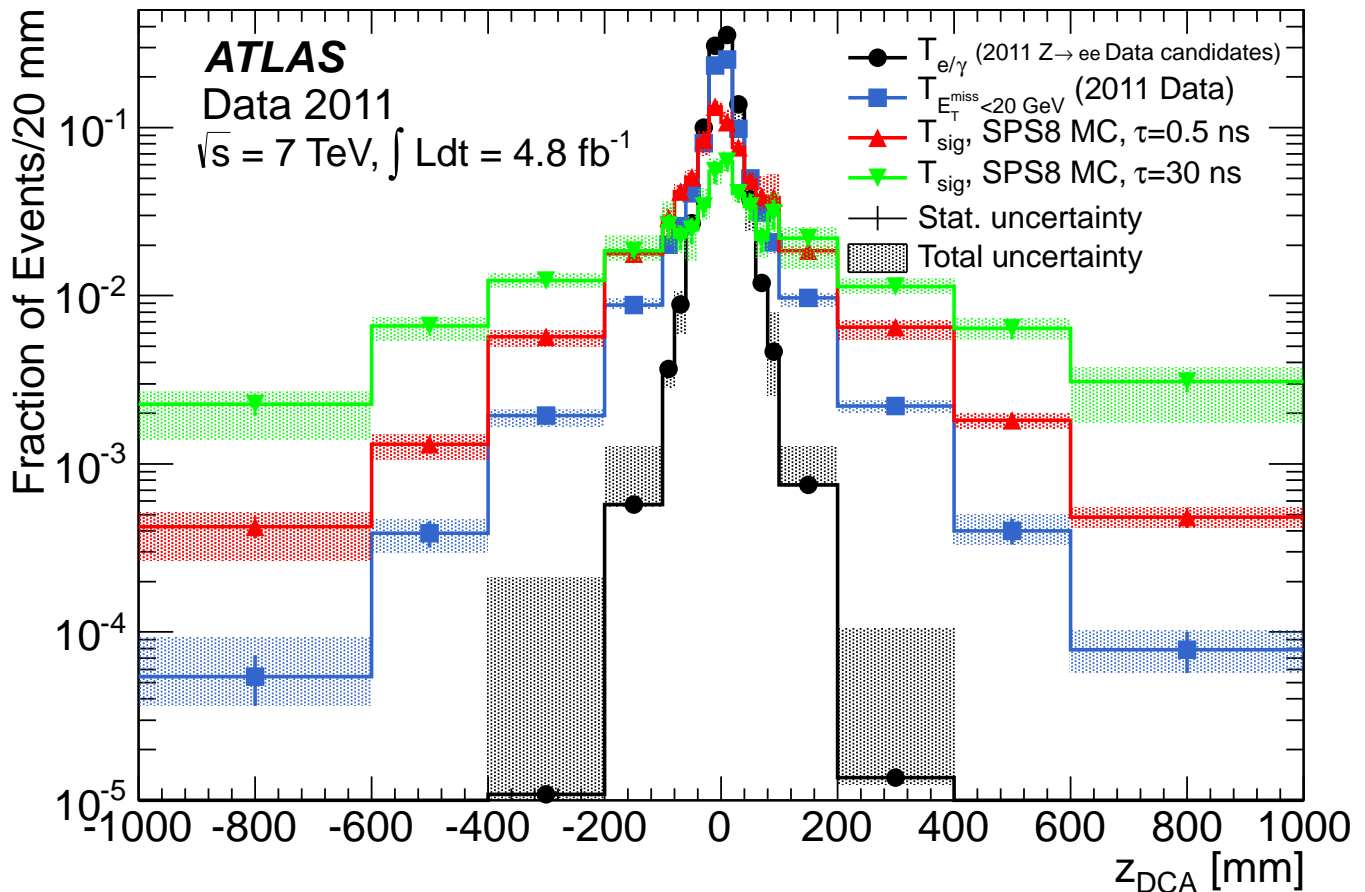


FIG. 3. The z_{DCA} templates from $Z \rightarrow ee$ events, from the TL control sample with $E_{\text{T}}^{\text{miss}}$ less than 20 GeV, and for MC simulations of GMSB signals with $\Lambda = 120$ TeV and values for the NLSP lifetime of $\tau = 0.5$ and 30 ns. The data points show the statistical errors, while the shaded bands show the total uncertainties, with statistical and systematic contributions added in quadrature. The first (last) bin includes the contribution from underflows (overflows).

60 GeV in the $E_{\text{T}}^{\text{miss}} < 20$ GeV control sample selects events with kinematic properties which are more similar to those of events in the signal region, and therefore the $E_{\text{T}} > 60$ GeV cut is applied to determine the nominal $T_{E_{\text{T}}^{\text{miss}} < 20 \text{ GeV}}$ template shape. Conservative possible systematic variations of this shape are taken to be the template shapes with E_{T} cuts of 50 GeV and 70 GeV on the photon candidates. The $T_{E_{\text{T}}^{\text{miss}} < 20 \text{ GeV}}$ template, along with its statistical and total uncertainties, is shown superimposed on Figure 3.

The distribution of arrival times of the photon candidates is used in the analysis as a cross-check. Figure 4 shows the timing distribution expected for selected signal events, for $\Lambda = 120$ TeV and for NLSP lifetime values of $\tau = 0.5$ and 30 ns. The expectations for the backgrounds are determined using the same data control samples described above. It is expected that the performance of the calorimeter timing measurement, as determined using the second-layer cell with the maximum deposited energy, should be rather insensitive to the details of the EM shower development. It was verified that the tim-

ing distribution of electrons in $Z \rightarrow ee$ events is very similar to that of loose photon candidates in the TL control sample with $E_{\text{T}}^{\text{miss}} < 20$ GeV. Therefore, the timing distribution determined with the larger $Z \rightarrow ee$ sample is characteristic of the timing performance expected for all prompt backgrounds, and is shown superimposed on Figure 4.

VII. SYSTEMATIC UNCERTAINTIES

When fitting the photon pointing distribution in data to the templates describing the expectations from signal and background, the total number of events is normalized to the 46 events observed in the data in the signal region. In addition, the background templates are determined using data. Thus, the analysis does not rely on predictions of the background normalization or composition, and there are therefore no systematic uncertainties to consider regarding the normalization of the backgrounds. As a result, the various systematic uncer-

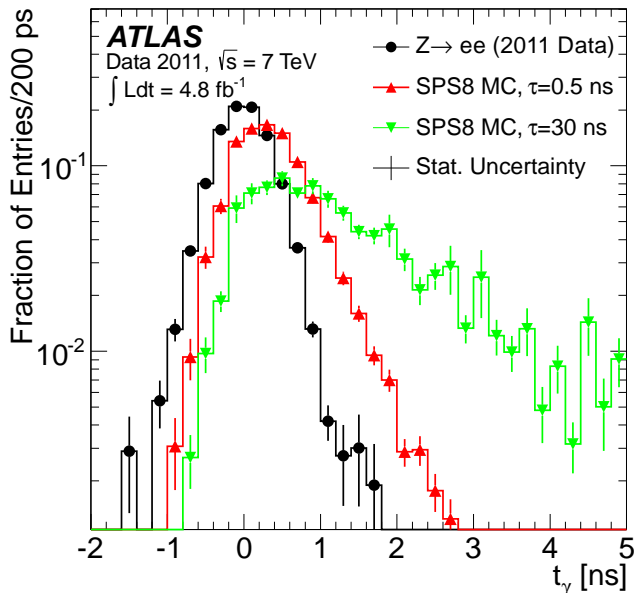


FIG. 4. The distribution of photon arrival times (t_γ) expected for SPS8 GMSB signal models with $\Lambda = 120$ TeV and for NLSP lifetime values of $\tau = 0.5$ and 30 ns. Superimposed is the expectation for prompt backgrounds, as determined using electrons from $Z \rightarrow ee$ events. The uncertainties shown are statistical only.

tainties relevant for the analysis can be divided into two types, namely “flat” uncertainties that are not a function of z_{DCA} but that affect the overall expected signal yield, and “shape” uncertainties related to the shapes of the unit-normalized signal and background pointing templates.

The shape uncertainties, which are correlated across z_{DCA} bins, are discussed in Sec. VI; their sizes within each bin are depicted in Fig. 3. The control region of TL events with $E_{\text{T}}^{\text{miss}}$ values in the intermediate range from 20 – 75 GeV is well described by a fit using the $T_{e/\gamma}$ and $T_{E_{\text{T}}^{\text{miss}} < 20 \text{ GeV}}$ distributions, providing further validation of the background template shapes and their associated systematic uncertainties.

The various flat systematic uncertainties are summarized in Table II, including the uncertainty on the integrated luminosity of $\pm 1.8\%$ [41]. The uncertainty on the trigger efficiency is $\pm 2.1\%$, which includes a contribution of $\pm 0.5\%$ for the determination of the diphoton trigger efficiency using a bootstrap method [42], and a contribution of $\pm 2\%$ taken as a conservative estimate of any possible dependence of the trigger efficiency on z_{DCA} or on the delay of signal photons. Uncertainties on the photon selection, the photon energy scale, and the detailed material composition of the detector, as described in Ref. [22], result in an uncertainty of $\pm 4.4\%$. The uncertainty due to the photon isolation requirement was estimated by varying the energy leakage and the pile-up corrections independently, resulting in an uncertainty of

$\pm 1.4\%$. Systematic uncertainties due to the $E_{\text{T}}^{\text{miss}}$ reconstruction, estimated by varying the cluster energies and the $E_{\text{T}}^{\text{miss}}$ resolution between the measured performance and MC expectations [39], contribute an uncertainty in the range of $\pm(1.1\text{--}8.2)\%$, with the higher uncertainty values applicable for lower values of Λ . As described in Sec. III, variations in the calculated NLO signal cross sections, times the signal acceptance and efficiency, at the level of $\pm(4.7\text{--}6.4)\%$ occur when varying the PDFs and factorization and renormalization scales. Adding these flat systematic uncertainties in quadrature gives a total systematic uncertainty on the signal yield in the range of $\pm(7.2\text{--}11.7)\%$, to which is added a contribution in the range of $\pm(0.7\text{--}5.0)\%$ due to statistical uncertainties in the signal MC predictions.

Source of Uncertainty	Value
Integrated Luminosity	$\pm 1.8\%$
Trigger Efficiency	$\pm 2.1\%$
Photon ID and E_{T} Scale/Resolution	$\pm 4.4\%$
Photon Isolation	$\pm 1.4\%$
$E_{\text{T}}^{\text{miss}}$: E_{T} Scale/Resolution	$\pm(1.1\text{--}8.2)\%$
Signal PDF and Scale Uncertainties	$\pm(4.7\text{--}6.4)\%$
Total Systematic Uncertainty	$\pm(7.2\text{--}11.7)\%$

TABLE II. Summary of systematic uncertainties on the total signal yield. The final row provides the total of these systematic uncertainties, calculated as the quadrature sum of the various contributions. There is an additional contribution, not shown in the Table, due to MC statistics, that ranges between $\pm 0.7\%$ and $\pm 5.0\%$, depending mostly on the NLSP lifetime.

VIII. RESULTS AND INTERPRETATION

The z_{DCA} distribution for the 46 loose photons of the events in the signal region with $E_{\text{T}}^{\text{miss}} > 75$ GeV is shown in Fig. 5. As expected for SM backgrounds, the distribution is rather narrow, and there is no obvious sign of a significant excess in the tails that would be expected for GMSB signal photons originating in the decays of long-lived neutralinos. There are three events with $|z_{\text{DCA}}| > 200$ mm, including one with a value of $z_{\text{DCA}} = +752$ mm. Some additional information about these three events is summarized in Table III.

The timing distribution for the 46 events in the signal region with $E_{\text{T}}^{\text{miss}} > 75$ GeV is shown in Fig. 6. The timing distribution is rather narrow, in agreement with the background-only expectation that is shown superimposed on Fig. 6, and there is no significant excess in the positive tail that would be expected for GMSB signal photons. The photon with the largest time value has $t \approx 1.2$ ns, and is measured using a calorimeter cell that was read out with medium gain. This photon corresponds to one of the three events with $|z_{\text{DCA}}| > 200$ mm that are described in Table III, but not to the most extreme pointing

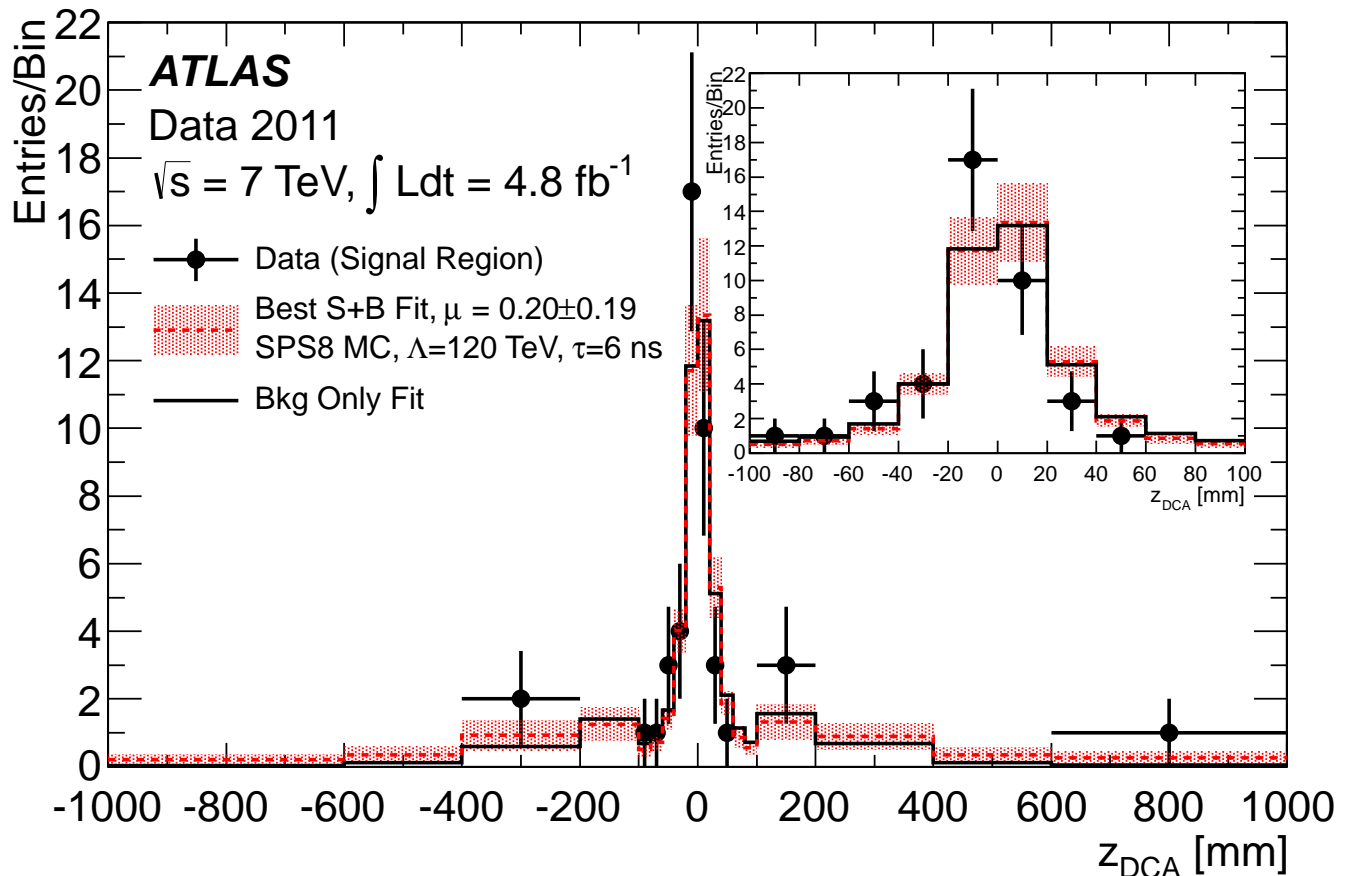


FIG. 5. The z_{DCA} distribution for the 46 loose photon candidates of the events in the signal region. Superimposed are the results of the background-only fit, as well as the results of the signal-plus-background fit for the case of $\Lambda = 120$ TeV and $\tau = 6$ ns. The hatching shows the total uncertainties in each bin for the signal-plus-background fit, for which the fitted signal strength is $\mu = 0.20 \pm 0.19$. The first (last) bin includes the contribution from underflows (overflows). The inset shows an expanded view of the central region, near $z_{\text{DCA}} = 0$.

Run	Event	$E_{\text{T}}^{\text{miss}}$	Loose Photon			Tight Photon		
Number	Number	(GeV)	E_{T} (GeV)	z_{DCA} (mm)	t_{γ} (ps)	E_{T} (GeV)	z_{DCA} (mm)	t_{γ} (ps)
186721	30399675	77.1	75.9	-274	360	72.0	22	580
187552	14929851	77.3	59.4	-262	1200	87.2	-120	240
191920	14157929	77.9	56.6	752	2	54.2	5	-200

TABLE III. Some parameters of the three “outlier” events mentioned in the text.

outlier. For the other two events in Table III, the timing is consistent with the hypothesis that the photon candidate is in-time.

To determine the final results, the pointing distribution shown in Fig. 5 is fitted using the pointing templates described previously. The binning shown in Fig. 5 is used in the fit. The background contribution is modeled in the fit as a weighted sum of the $T_{e/\gamma}$ and $T_{E_{\text{T}}^{\text{miss}} < 20 \text{ GeV}}$ templates. Background-only fits are performed to determine the compatibility of the observed pointing distribution with the background-only hypothesis. Signal-plus-

background fits are performed to determine, via profile likelihood fits, the 95% CL limit on the signal strength, μ , defined as the number of fitted signal events divided by the SPS8 expectation for the signal yield. In both cases, the overall normalization is constrained to the 46 events observed in the signal region in data, and the relative weighting of the two background templates is treated as a nuisance parameter in the fit.

Table IV shows the number of observed events in the various bins of z_{DCA} shown in Fig. 5, except that the number of z_{DCA} bins is reduced for display pur-

Fit Type	Event Type	Range of $ z_{\text{DCA}} $ values [mm]									
		0-20	20-40	40-60	60-80	80-100	100-200	200-400	400-600	> 600	
-	Data	27	7	4	1	1	3	2	0	1	
Bkg Only	Bkg	25.0±2.2	9.1±0.8	3.8±0.3	2.1±0.5	1.4±0.4	3.0±1.1	1.3±0.5	0.2±0.1	0.08±0.03	
Signal Plus	Total	25.1±4.2	9.3±1.5	3.3±0.7	1.6±0.6	1.1±0.4	2.6±1.0	1.8±0.8	0.7±0.5	0.5±0.4	
	Sig	0.7±0.6	0.5±0.5	0.4±0.3	0.3±0.3	0.3±0.3	1.2±1.1	1.3±1.2	0.6±0.5	0.4±0.4	
	Bkg	24.4±4.2	8.8±1.5	2.9±0.8	1.3±0.7	0.8±0.6	1.4±1.5	0.5±0.7	0.1±0.1	0.03±0.04	

TABLE IV. Integrals over various $|z_{\text{DCA}}|$ ranges of the distributions shown in Fig. 5 for the 46 loose photon candidates in the signal region. The numbers of events observed in data are shown, as well as the results of a background-only fit and a signal-plus-background fit for the case of $\Lambda = 120$ TeV and $\tau = 6$ ns. The fitted signal strength is $\mu = 0.20 \pm 0.19$. The errors shown correspond to the sum of statistical and systematic uncertainties. The numbers of signal and background events from the signal-plus-background fit are negatively correlated.

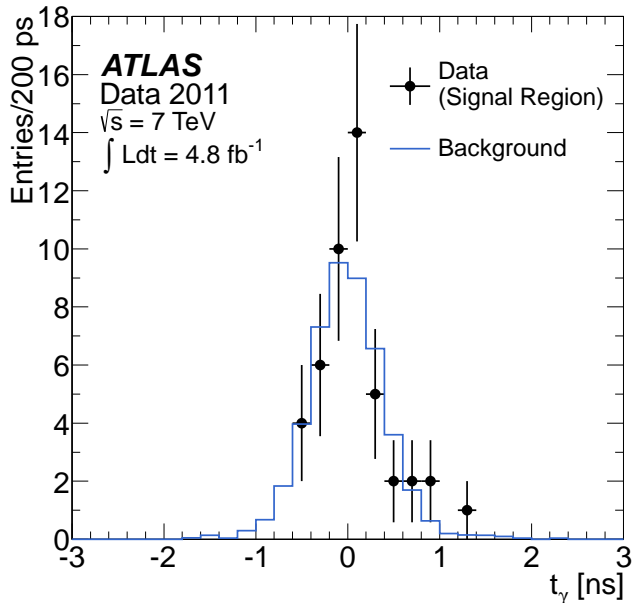


FIG. 6. The distribution of arrival times (t_γ) for the 46 loose photon candidates of the events in the signal region. Superimposed for comparison is the shape of the timing distribution expected for background only, normalized to 46 total events.

poses by a factor of two by taking the absolute value of z_{DCA} . Included in Table IV are the results from the background-only and signal-plus-background fit, for the case of $\Lambda = 120$ TeV and $\tau = 6$ ns. Comparing the first two rows of Table IV shows that there is fair agreement between the observed data and the results of the background-only fit, though there is some excess seen in the data for larger $|z_{\text{DCA}}|$ values. The p_0 value for the background-only hypothesis is ≈ 0.060 , indicating that the slight excess has a significance equivalent to $\approx 1.5\sigma$. The excess is dominated by the outlier photon with $z_{\text{DCA}} = 752$ mm; removing this event from the distribution and performing a new fit, one obtains a p_0 value of ≈ 0.30 , indicating in this case a much better

agreement with the background-only model.

The last three rows of Table IV show the results of the signal-plus-background fit for the case of $\Lambda = 120$ TeV and $\tau = 6$ ns, including the total number of fitted events in each $|z_{\text{DCA}}|$ bin, as well as the separate contributions from signal and from background. For this case, the signal-plus-background fit returns a central value for the signal strength of $\mu = 0.20 \pm 0.19$, and the fitted value of the nuisance parameter specifying the fraction of the background that is attributed to the $T_{E_{\text{T}}^{\text{miss}} < 20 \text{ GeV}}$ template is 0.32 ± 0.38 . The fit results are used to determine, via the CLs method [43], 95% CL limits on the number of signal events. The results, derived within the RooStats framework [44], are determined for both the observed limit, where the fit is performed to the pointing distribution of the 46 observed events in the signal region, and for the expected limit, where the fit is performed to ensembles of pseudo-experiments generated according to the background-only hypothesis. The slight excess for larger $|z_{\text{DCA}}|$ values leads to a result where the observed limit on the number of signal events is somewhat less restrictive than the expected limit. For the example of $\Lambda = 120$ TeV and $\tau = 6$ ns, the observed (expected) 95% CL limit is 18.3 (9.8) signal events.

By repeating the statistical procedure for various Λ and τ values, the limits are determined as a function of these SPS8 model parameters. The left plot of Fig. 7 shows the 95% CL limits on the number of signal events versus τ , for the case with $\Lambda = 120$ TeV. The right plot of Fig. 7 shows the 95% CL limits on the allowed cross section versus τ , also for the case with $\Lambda = 120$ TeV. Each plot includes a curve indicating the SPS8 theory prediction for $\Lambda = 120$ TeV. The intersections where the limits cross the theory prediction show that, for $\Lambda = 120$ TeV, values of τ below 8.7 ns are excluded at 95% CL, whereas the expected limit would exclude values of τ below 14.6 ns.

Comparing with the theoretical cross section of the SPS8 GMSB model, the results are converted into an exclusion region in the two-dimensional plane of τ versus Λ , as shown in Fig. 8. Also shown in the figure are corre-

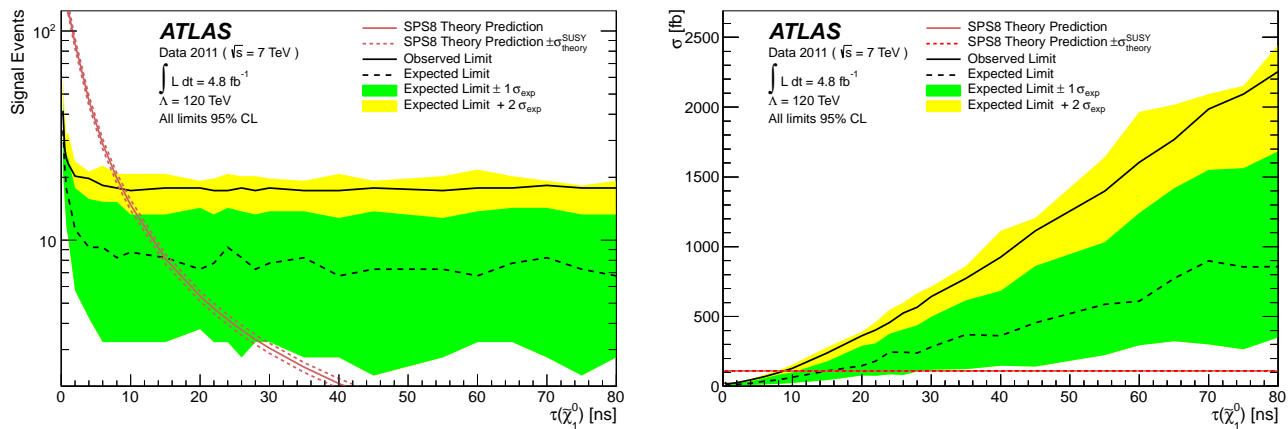


FIG. 7. 95% CL limits on (left) the number of signal events and (right) the SPS8 signal cross section, as a function of NLSP lifetime, for the case of $\Lambda = 120$ TeV. The region below the limit curve is excluded at 95% CL.

sponding limits on the lifetime versus the masses of the lightest neutralino and lightest charginos, where the relation between Λ and sparticle masses is taken from the theory.

IX. CONCLUSIONS

A search has been performed for non-pointing photons in the diphoton plus E_T^{miss} final state, using the full data sample of 7 TeV pp collisions recorded in 2011 with the ATLAS detector at the LHC. The analysis uses the capability of the ATLAS LAr calorimeter to measure the flight direction of photons to perform the search, with the precision measurement of the arrival time of photons used as a cross-check of the results.

No significant evidence for non-pointing photons is observed. Interpreted in the context of the GMSB SPS8 benchmark model, the results provide 95% CL exclusion limits in the plane of τ (the lifetime of the lightest neutralino) versus Λ (the effective scale of SUSY breaking) or, alternatively, versus the mass of the lightest neutralino. For example, for $\Lambda = 70$ TeV (160 TeV), NLSP lifetimes between 0.25 and 50.7 ns (2.7 ns) are excluded at 95% CL.

X. ACKNOWLEDGEMENTS

We thank CERN for the very successful operation of the LHC, as well as the support staff from our institutions without whom ATLAS could not be operated efficiently.

We acknowledge the support of ANPCyT, Argentina; YerPhI, Armenia; ARC, Australia; BMWF and FWF, Austria; ANAS, Azerbaijan; SSTC, Belarus; CNPq and FAPESP, Brazil; NSERC, NRC and CFI, Canada; CERN; CONICYT, Chile; CAS, MOST and NSFC, China; COLCIENCIAS, Colombia; MSMT CR, MPO CR and VSC CR, Czech Republic; DNRF, DNSRC and Lundbeck Foundation, Denmark; EPLANET, ERC and NSRF, European Union; IN2P3-CNRS, CEA-DSM/IRFU, France; GNSF, Georgia; BMBF, DFG, HGF, MPG and AvH Foundation, Germany; GSRT and NSRF, Greece; ISF, MINERVA, GIF, DIP and Benoziyo Center, Israel; INFN, Italy; MEXT and JSPS, Japan; CNRST, Morocco; FOM and NWO, Netherlands; BRF and RCN, Norway; MNiSW, Poland; GRICES and FCT, Portugal; MERYS (MECTS), Romania; MES of Russia and ROSATOM, Russian Federation; JINR; MSTB, Serbia; MSSR, Slovakia; ARRS and MIZŠ, Slovenia; DST/NRF, South Africa; MICINN, Spain; SRC and Wallenberg Foundation, Sweden; SER, SNSF and Cantons of Bern and Geneva, Switzerland; NSC, Taiwan; TAEK, Turkey; STFC, the Royal Society and Leverhulme Trust, United Kingdom; DOE and NSF, United States of America.

The crucial computing support from all WLCG partners is acknowledged gratefully, in particular from CERN and the ATLAS Tier-1 facilities at TRIUMF (Canada), NDGF (Denmark, Norway, Sweden), CC-IN2P3 (France), KIT/GridKA (Germany), INFN-CNAF (Italy), NL-T1 (Netherlands), PIC (Spain), ASGC (Taiwan), RAL (UK) and BNL (USA) and in the Tier-2 facilities worldwide.

[1] H. Miyazawa, Prog. Theor. Phys. **36** (6), 1266 (1966).
 [2] P. Ramond, Phys. Rev. **D3**, 2415 (1971).

[3] Y. A. Golfand and E. P. Likhtman, JETP Lett. **13**, 323 (1971).

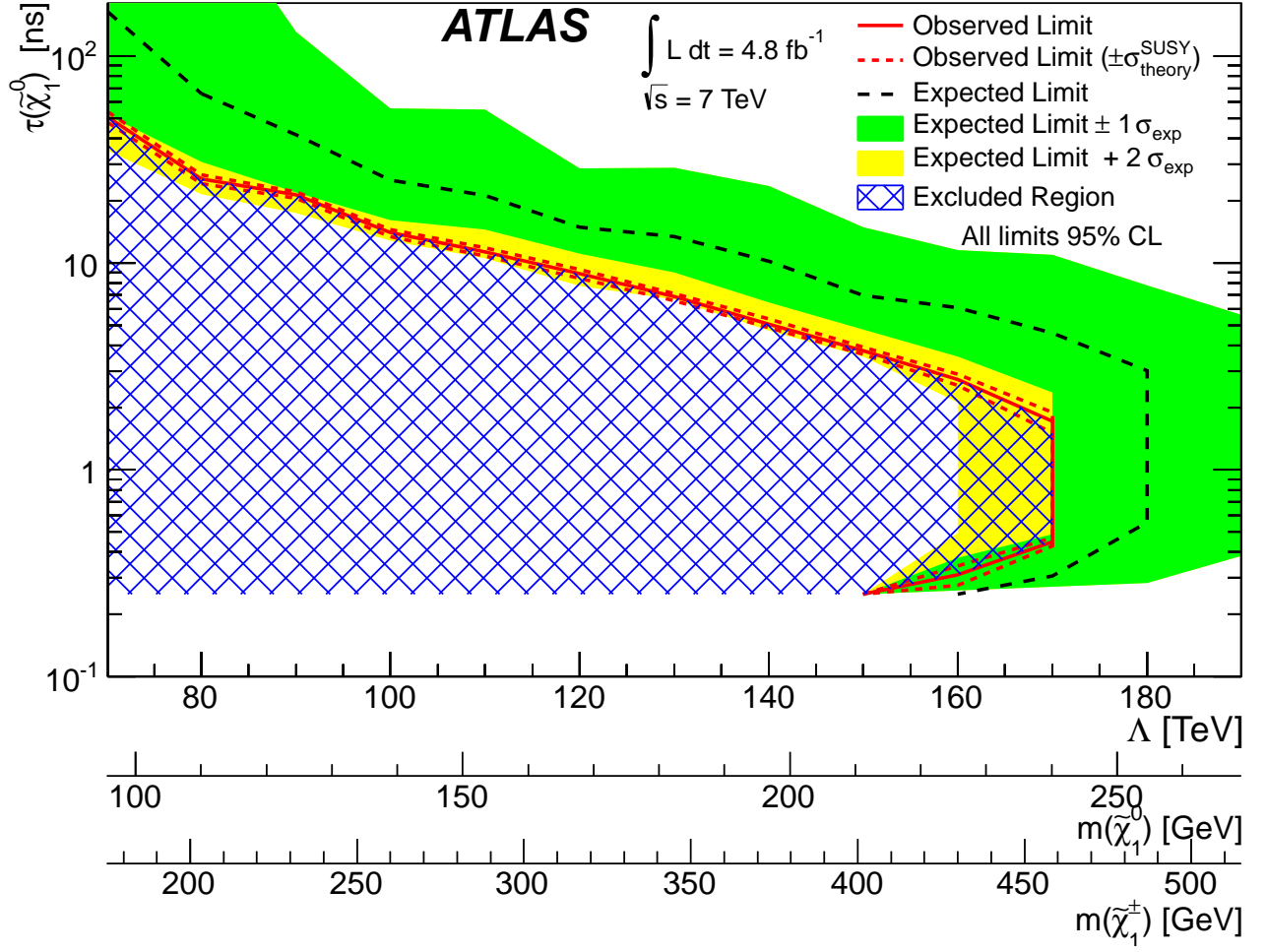


FIG. 8. The expected and observed limits in the plane of NLSP lifetime versus Λ (and also versus the $\tilde{\chi}_1^0$ or $\tilde{\chi}_1^\pm$ masses), for the SPS8 model. Linear interpolations are shown to connect between Λ values, separated by 10 TeV, for which MC signal samples are available. The region excluded at 95% CL is shown as the blue hatched area. The limit is not shown below an NLSP lifetime of 0.25 ns, which, due to the MC signal samples available, is the smallest value considered in the analysis. The green and yellow bands show the $\pm 1\sigma$ and $+2\sigma$ variations, respectively, around the expected limit. The -2σ variation is not shown since it would correspond to a negative number of expected signal events, which is unphysical.

- [4] A. Neveu and J. H. Schwarz, Nucl. Phys. B **31**, 86 (1971).
 [5] A. Neveu and J. H. Schwarz, Phys. Rev. D **4**, 1109 (1971).
 [6] J.-L. Gervais and B. Sakita, Nucl. Phys. B **34**, 632 (1971).
 [7] D. V. Volkov and V. P. Akulov, Phys. Lett. B **46**, 109 (1973).
 [8] J. Wess and B. Zumino, Phys. Lett. B **49**, 52 (1974).
 [9] J. Wess and B. Zumino, Nucl. Phys. B **70**, 39 (1974).
 [10] P. Fayet, Phys. Lett. B **64**, 159 (1976).
 [11] P. Fayet, Phys. Lett. B **69**, 489 (1977).
 [12] G. R. Farrar and P. Fayet, Phys. Lett. B **76**, 575 (1978).
 [13] P. Fayet, Phys. Lett. B **84**, 416 (1979).
 [14] S. Dimopoulos and H. Georgi, Nucl. Phys. B **193**, 150 (1981).
 [15] M. Dine and W. Fischler, Phys. Lett. B **110**, 227 (1982).
 [16] L. Alvarez-Gaum, M. Claudson, and M. B. Wise, Nucl. Phys. B **207**, 96 (1982).
 [17] C. R. Nappi and B. A. Ovrut, Phys. Lett. B **113**, 175 (1982).
 [18] M. Dine and A. Nelson, Phys. Rev. D **48**, 1277 (1993), hep-ph/9303230.
 [19] M. Dine, A. Nelson, and Y. Shirman, Phys. Rev. D **51**, 1362 (1995), hep-ph/9408384.
 [20] M. Dine, A. Nelson, Y. Nir, and Y. Shirman, Phys. Rev. D **53**, 2658 (1996), hep-ph/9507378.
 [21] B. C. Allanach et al., Eur. Phys. J. C **25**, 113 (2002), hep-ph/0202233.
 [22] ATLAS Collaboration, Phys. Lett. B **718**, 411 (2012), arXiv:1209.0753 [hep-ex].
 [23] CMS Collaboration, arXiv:1212.1838 [hep-ex].
 [24] ATLAS Collaboration, JINST **3**, S08003 (2008).
 [25] ATLAS Collaboration, Phys. Lett. B **716**, 1 (2012), arXiv:1207.7214 [hep-ex].
 [26] N. Buchanan et al., JINST **3**, P03004 (2008).

[27] H. Abreu et al., JINST **5**, P09003 (2010).
 [28] M. Aharrouche et al., Nucl. Instrum. Meth. A **597**, 178 (2008).
 [29] F. E. Paige, S. D. Protopopescu, H. Baer, and X. Tata, hep-ph/0312045.
 [30] W. Beenakker, R. Hopker, and M. Spira, hep-ph/9611232.
 [31] P. M. Nadolsky et al., Phys. Rev. D **78**, 013004 (2008), arXiv:0802.0007 [hep-ph].
 [32] M. Kramer et al., arXiv:1206.2892 [hep-ph].
 [33] M. Bahr et al., Eur. Phys. J. C **58**, 639 (2008), arXiv:0803.0883 [hep-ph].
 [34] A. Sherstnev and R. S. Thorne, Eur. Phys. J. C **55**, 553 (2008), arXiv:0711.2473 [hep-ph].
 [35] ATLAS Collaboration, Eur. Phys. J. C **70**, 823 (2010), arXiv:1005.4568 [physics.ins-det].
 [36] GEANT4 Collaboration, S. Agostinelli et al., Nucl. Instrum. Meth. A **506**, 250 (2003).
 [37] ATLAS Collaboration, Phys.Rev. D **83**, 052005 (2011), arXiv:1012.4389 [hep-ex].
 [38] ATLAS Collaboration, Eur. Phys. J. C **72**, 1909 (2012), arXiv:1110.3174 [hep-ex].
 [39] ATLAS Collaboration, Eur. Phys. J. C **72**, 1844 (2012), arXiv:1108.5602 [hep-ex].
 [40] ATLAS Collaboration, Phys. Lett. B **710**, 519 (2012), arXiv:1111.4116 [hep-ex].
 [41] ATLAS Collaboration, arXiv:1302.4393 [hep-ex].
 [42] ATLAS Collaboration, Eur. Phys. J. C **72**, 1849 (2012), arXiv:1110.1530 [hep-ex].
 [43] A. L. Read, J. Phys. G **28**, 2693 (2002).
 [44] L. Moneta et al., PoS **ACAT2010** (2010) 057, arXiv:1009.1003 [physics.data-an].

The ATLAS Collaboration

G. Aad⁴⁸, T. Abajyan²¹, B. Abbott¹¹², J. Abdallah¹², S. Abdel Khalek¹¹⁶, A.A. Abdelalim⁴⁹, O. Abidinov¹¹, R. Aben¹⁰⁶, B. Abi¹¹³, M. Abolins⁸⁹, O.S. AbouZeid¹⁵⁹, H. Abramowicz¹⁵⁴, H. Abreu¹³⁷, Y. Abulaiti^{147a,147b}, B.S. Acharya^{165a,165b,a}, L. Adamczyk^{38a}, D.L. Adams²⁵, T.N. Addy⁵⁶, J. Adelman¹⁷⁷, S. Adomeit⁹⁹, T. Adye¹³⁰, S. Aefsky²³, J.A. Aguilar-Saavedra^{125b,b}, M. Agustoni¹⁷, S.P. Ahlen²², F. Ahles⁴⁸, A. Ahmad¹⁴⁹, M. Ahsan⁴¹, G. Aielli^{134a,134b}, T.P.A. Åkesson⁸⁰, G. Akimoto¹⁵⁶, A.V. Akimov⁹⁵, M.A. Alam⁷⁶, J. Albert¹⁷⁰, S. Albrand⁵⁵, M.J. Alconada Verzini⁷⁰, M. Aleksa³⁰, I.N. Aleksandrov⁶⁴, F. Alessandria^{90a}, C. Alexa^{26a}, G. Alexander¹⁵⁴, G. Alexandre⁴⁹, T. Alexopoulos¹⁰, M. Alhroob^{165a,165c}, M. Aliev¹⁶, G. Alimonti^{90a}, J. Alison³¹, B.M.M. Allbrooke¹⁸, L.J. Allison⁷¹, P.P. Allport⁷³, S.E. Allwood-Spiers⁵³, J. Almond⁸³, A. Aloisio^{103a,103b}, R. Alon¹⁷³, A. Alonso³⁶, F. Alonso⁷⁰, A. Altheimer³⁵, B. Alvarez Gonzalez⁸⁹, M.G. Alviggi^{103a,103b}, K. Amako⁶⁵, Y. Amaral Coutinho^{24a}, C. Amelung²³, V.V. Ammosov^{129,*}, S.P. Amor Dos Santos^{125a}, A. Amorim^{125a,c}, S. Amoroso⁴⁸, N. Amram¹⁵⁴, C. Anastopoulos³⁰, L.S. Ancu¹⁷, N. Andari³⁰, T. Andeen³⁵, C.F. Anders^{58b}, G. Anders^{58a}, K.J. Anderson³¹, A. Andreazza^{90a,90b}, V. Andrei^{58a}, X.S. Anduaga⁷⁰, S. Angelidakis⁹, P. Anger⁴⁴, A. Angerami³⁵, F. Anghinolfi³⁰, A. Anisenkov¹⁰⁸, N. Anjos^{125a}, A. Annovi⁴⁷, A. Antonaki⁹, M. Antonelli⁴⁷, A. Antonov⁹⁷, J. Antos^{145b}, F. Anulli^{133a}, M. Aoki¹⁰², L. Aperio Bella¹⁸, R. Apolle^{119,d}, G. Arabidze⁸⁹, I. Aracena¹⁴⁴, Y. Arai⁶⁵, A.T.H. Arce⁴⁵, S. Arfaoui¹⁴⁹, J-F. Arguin⁹⁴, S. Argyropoulos⁴², E. Arik^{19a,*}, M. Arik^{19a}, A.J. Armbruster⁸⁸, O. Arnaez⁸², V. Arnal⁸¹, A. Artamonov⁹⁶, G. Artoni^{133a,133b}, D. Arutinov²¹, S. Asai¹⁵⁶, N. Asbah⁹⁴, S. Ask²⁸, B. Åsman^{147a,147b}, L. Asquith⁶, K. Assamagan²⁵, R. Astalos^{145a}, A. Astbury¹⁷⁰, M. Atkinson¹⁶⁶, B. Auerbach⁶, E. Auge¹¹⁶, K. Augsten¹²⁷, M. Auroousseau^{146b}, G. Avolio³⁰, D. Axen¹⁶⁹, G. Azuelos^{94,e}, Y. Azuma¹⁵⁶, M.A. Baak³⁰, G. Baccaglioni^{90a}, C. Bacci^{135a,135b}, A.M. Bach¹⁵, H. Bachacou¹³⁷, K. Bachas¹⁵⁵, M. Backes⁴⁹, M. Backhaus²¹, J. Backus Mayes¹⁴⁴, E. Badescu^{26a}, P. Bagiacchi^{133a,133b}, P. Bagnaia^{133a,133b}, Y. Bai^{33a}, D.C. Bailey¹⁵⁹, T. Bain³⁵, J.T. Baines¹³⁰, O.K. Baker¹⁷⁷, S. Baker⁷⁷, P. Balek¹²⁸, F. Balli¹³⁷, E. Banas³⁹, P. Banerjee⁹⁴, Sw. Banerjee¹⁷⁴, D. Banfi³⁰, A. Bangert¹⁵¹, V. Bansal¹⁷⁰, H.S. Bansil¹⁸, L. Barak¹⁷³, S.P. Baranov⁹⁵, T. Barber⁴⁸, E.L. Barberio⁸⁷, D. Barberis^{50a,50b}, M. Barbero⁸⁴, D.Y. Bardin⁶⁴, T. Barillari¹⁰⁰, M. Barisonzi¹⁷⁶, T. Barklow¹⁴⁴, N. Barlow²⁸, B.M. Barnett¹³⁰, R.M. Barnett¹⁵, A. Baroncelli^{135a}, G. Barone⁴⁹, A.J. Barr¹¹⁹, F. Barreiro⁸¹, J. Barreiro Guimarães da Costa⁵⁷, R. Bartoldus¹⁴⁴, A.E. Barton⁷¹, V. Bartsch¹⁵⁰,

- A. Basye¹⁶⁶, R.L. Bates⁵³, L. Batkova^{145a},
 J.R. Batley²⁸, A. Battaglia¹⁷, M. Battistin³⁰,
 F. Bauer¹³⁷, H.S. Bawa^{144.f}, S. Beale⁹⁹, T. Beau⁷⁹,
 P.H. Beauchemin¹⁶², R. Beccherle^{50a}, P. Bechtle²¹,
 H.P. Beck¹⁷, K. Becker¹⁷⁶, S. Becker⁹⁹,
 M. Beckingham¹³⁹, K.H. Becks¹⁷⁶, A.J. Beddall^{19c},
 A. Beddall^{19c}, S. Bedikian¹⁷⁷, V.A. Bednyakov⁶⁴,
 C.P. Bee⁸⁴, L.J. Beemster¹⁰⁶, T.A. Beermann¹⁷⁶,
 M. Begel²⁵, C. Belanger-Champagne⁸⁶, P.J. Bell⁴⁹,
 W.H. Bell⁴⁹, G. Bella¹⁵⁴, L. Bellagamba^{20a},
 A. Bellerive²⁹, M. Bellomo³⁰, A. Belloni⁵⁷,
 O. Beloborodova^{108.g}, K. Belotskiy⁹⁷, O. Beltramello³⁰,
 O. Benary¹⁵⁴, D. Benchekroun^{136a}, K. Bendtz^{147a,147b},
 N. Benekos¹⁶⁶, Y. Benhammou¹⁵⁴,
 E. Benhar Nocchioli⁴⁹, J.A. Benitez Garcia^{160b},
 D.P. Benjamin⁴⁵, J.R. Bensinger²³, K. Benslama¹³¹,
 S. Bentvelsen¹⁰⁶, D. Berge³⁰, E. Bergeaas Kuutmann¹⁶,
 N. Berger⁵, F. Berghaus¹⁷⁰, E. Berglund¹⁰⁶,
 J. Beringer¹⁵, P. Bernat⁷⁷, R. Bernhard⁴⁸, C. Bernius⁷⁸,
 F.U. Bernlochner¹⁷⁰, T. Berry⁷⁶, C. Bertella⁸⁴,
 F. Bertolucci^{123a,123b}, M.I. Besana^{90a,90b},
 G.J. Besjes¹⁰⁵, N. Besson¹³⁷, S. Bethke¹⁰⁰,
 R. Bhandari³⁵, W. Bhimji⁴⁶, R.M. Bianchi³⁰,
 L. Bianchini²³, M. Bianco^{72a,72b}, O. Biebel⁹⁹,
 S.P. Bieniek⁷⁷, K. Bierwagen⁵⁴, J. Biesiada¹⁵,
 M. Biglietti^{135a}, H. Bilokon⁴⁷, M. Bindi^{20a,20b},
 S. Binet¹¹⁶, A. Bingul^{19c}, C. Bini^{133a,133b}, B. Bittner¹⁰⁰,
 C.W. Black¹⁵¹, J.E. Black¹⁴⁴, K.M. Black²²,
 D. Blackburn¹³⁹, R.E. Blair⁶, J.-B. Blanchard¹³⁷,
 T. Blazek^{145a}, I. Bloch⁴², C. Blocker²³, J. Blocki³⁹,
 W. Blum⁸², U. Blumenschein⁵⁴, G.J. Bobbink¹⁰⁶,
 V.S. Bobrovnikov¹⁰⁸, S.S. Bocchetta⁸⁰, A. Bocci⁴⁵,
 C.R. Boddy¹¹⁹, M. Boehler⁴⁸, J. Boek¹⁷⁶, T.T. Boek¹⁷⁶,
 N. Boelaert³⁶, J.A. Bogaerts³⁰, A. Bogdanchikov¹⁰⁸,
 A. Bogouch^{91,*}, C. Bohm^{147a}, J. Bohm¹²⁶,
 V. Boisvert⁷⁶, T. Bold^{38a}, V. Boldea^{26a}, N.M. Bolnet¹³⁷,
 M. Bomben⁷⁹, M. Bona⁷⁵, M. Boonekamp¹³⁷,
 S. Bordini⁷⁹, C. Borer¹⁷, A. Borisov¹²⁹, G. Borissov⁷¹,
 M. Borri⁸³, S. Borroni⁴², J. Bortfeldt⁹⁹,
 V. Bortolotto^{135a,135b}, K. Bos¹⁰⁶, D. Boscherini^{20a},
 M. Bosman¹², H. Boterenbrood¹⁰⁶, J. Bouchami⁹⁴,
 J. Boudreau¹²⁴, E.V. Bouhova-Thacker⁷¹,
 D. Boumediene³⁴, C. Bourdarios¹¹⁶, N. Bousson⁸⁴,
 S. Boutouil^{136d}, A. Boveia³¹, J. Boyd³⁰, I.R. Boyko⁶⁴,
 I. Bozovic-Jelisavcic^{13b}, J. Bracinik¹⁸, P. Branchini^{135a},
 A. Brandt⁸, G. Brandt¹⁵, O. Brandt⁵⁴, U. Bratzler¹⁵⁷,
 B. Brau⁸⁵, J.E. Brau¹¹⁵, H.M. Braun^{176,*},
 S.F. Brazzale^{165a,165c}, B. Brelrier¹⁵⁹, J. Bremer³⁰,
 K. Brendlinger¹²¹, R. Brenner¹⁶⁷, S. Bressler¹⁷³,
 T.M. Bristow^{146c}, D. Britton⁵³, F.M. Brochu²⁸,
 I. Brock²¹, R. Brock⁸⁹, F. Broggi^{90a}, C. Bromberg⁸⁹,
 J. Bronner¹⁰⁰, G. Brooijmans³⁵, T. Brooks⁷⁶,
 W.K. Brooks^{32b}, G. Brown⁸³,
 P.A. Bruckman de Renstrom³⁹, D. Bruncko^{145b},
 R. Bruneliere⁴⁸, S. Brunet⁶⁰, A. Bruni^{20a}, G. Bruni^{20a},
 M. Bruschi^{20a}, L. Bryngemark⁸⁰, T. Buanes¹⁴,
 Q. Buat⁵⁵, F. Bucci⁴⁹, J. Buchanan¹¹⁹, P. Buchholz¹⁴²,
 R.M. Buckingham¹¹⁹, A.G. Buckley⁴⁶, S.I. Buda^{26a},
 I.A. Budagov⁶⁴, B. Budick¹⁰⁹, L. Bugge¹¹⁸,
 O. Bulekov⁹⁷, A.C. Bundock⁷³, M. Bunse⁴³,
 T. Buran^{118,*}, H. Burckhart³⁰, S. Burdin⁷³,
 T. Burgess¹⁴, S. Burke¹³⁰, E. Busato³⁴, V. Büscher⁸²,
 P. Bussey⁵³, C.P. Buszello¹⁶⁷, B. Butler⁵⁷,
 J.M. Butler²², C.M. Buttar⁵³, J.M. Butterworth⁷⁷,
 W. Buttinger²⁸, M. Byszewski¹⁰, S. Cabrera Urbán¹⁶⁸,
 D. Caforio^{20a,20b}, O. Cakir^{4a}, P. Calafiura¹⁵,
 G. Calderini⁷⁹, P. Calfayan⁹⁹, R. Calkins¹⁰⁷,
 L.P. Caloba^{24a}, R. Caloi^{133a,133b}, D. Calvet³⁴,
 S. Calvet³⁴, R. Camacho Toro⁴⁹, P. Camarri^{134a,134b},
 D. Cameron¹¹⁸, L.M. Caminada¹⁵,
 R. Caminal Armadans¹², S. Campana³⁰,
 M. Campanelli⁷⁷, V. Canale^{103a,103b}, F. Canelli³¹,
 A. Canepa^{160a}, J. Cantero⁸¹, R. Cantrill⁷⁶, T. Cao⁴⁰,
 M.D.M. Capeans Garrido³⁰, I. Caprini^{26a},
 M. Caprini^{26a}, D. Capriotti¹⁰⁰, M. Capua^{37a,37b},
 R. Caputo⁸², R. Cardarelli^{134a}, T. Carli³⁰,
 G. Carlino^{103a}, L. Carminati^{90a,90b}, S. Caron¹⁰⁵,
 E. Carquin^{32b}, G.D. Carrillo-Montoya^{146c},
 A.A. Carter⁷⁵, J.R. Carter²⁸, J. Carvalho^{125a,h},
 D. Casadei¹⁰⁹, M.P. Casado¹², M. Cascella^{123a,123b},
 C. Caso^{50a,50b,*}, E. Castaneda-Miranda¹⁷⁴,
 A. Castelli¹⁰⁶, V. Castillo Gimenez¹⁶⁸, N.F. Castro^{125a},
 G. Cataldi^{72a}, P. Catastini⁵⁷, A. Catinaccio³⁰,
 J.R. Catmore³⁰, A. Cattai³⁰, G. Cattani^{134a,134b},
 S. Caughron⁸⁹, V. Cavaliere¹⁶⁶, D. Cavalli^{90a},
 M. Cavalli-Sforza¹², V. Cavaiani^{123a,123b},
 F. Ceradini^{135a,135b}, B. Cerio⁴⁵, A.S. Cerqueira^{24b},
 A. Cerri¹⁵, L. Cerrito⁷⁵, F. Cerutti¹⁵, A. Cervelli¹⁷,
 S.A. Cetin^{19b}, A. Chafaq^{136a}, D. Chakraborty¹⁰⁷,
 I. Chalupkova¹²⁸, K. Chan³, P. Chang¹⁶⁶,
 B. Chapleau⁸⁶, J.D. Chapman²⁸, J.W. Chapman⁸⁸,
 D.G. Charlton¹⁸, V. Chavda⁸³, C.A. Chavez Barajas³⁰,
 S. Cheatham⁸⁶, S. Chekanov⁶, S.V. Chekulaev^{160a},
 G.A. Chelkov⁶⁴, M.A. Chelstowska¹⁰⁵, C. Chen⁶³,
 H. Chen²⁵, S. Chen^{33c}, X. Chen¹⁷⁴, Y. Chen³⁵,
 Y. Cheng³¹, A. Cheplakov⁶⁴,
 R. Cherkaoui El Moursli^{136e}, V. Chernyatin²⁵,
 E. Cheu⁷, S.L. Cheung¹⁵⁹, L. Chevalier¹³⁷,
 V. Chiarella⁴⁷, G. Chiefari^{103a,103b}, J.T. Childers³⁰,
 A. Chilingarov⁷¹, G. Chiodini^{72a}, A.S. Chisholm¹⁸,
 R.T. Chislett⁷⁷, A. Chitan^{26a}, M.V. Chizhov⁶⁴,
 G. Choudalakis³¹, S. Chouridou⁹, B.K.B. Chow⁹⁹,
 I.A. Christidi⁷⁷, A. Christov⁴⁸,
 D. Chromek-Burckhart³⁰, M.L. Chu¹⁵², J. Chudoba¹²⁶,
 G. Ciapetti^{133a,133b}, A.K. Ciftci^{4a}, R. Ciftci^{4a},
 D. Cinca⁶², V. Cindro⁷⁴, A. Ciocio¹⁵, M. Cirilli⁸⁸,
 P. Cirkovic^{13b}, Z.H. Citron¹⁷³, M. Citterio^{90a},
 M. Ciubancan^{26a}, A. Clark⁴⁹, P.J. Clark⁴⁶,
 R.N. Clarke¹⁵, J.C. Clemens⁸⁴, B. Clement⁵⁵,
 C. Clement^{147a,147b}, Y. Coadou⁸⁴, M. Cobal^{165a,165c},
 A. Coccaro¹³⁹, J. Cochran⁶³, S. Coelli^{90a}, L. Coffey²³,
 J.G. Cogan¹⁴⁴, J. Coggeshall¹⁶⁶, J. Colas⁵, S. Cole¹⁰⁷,
 A.P. Colijn¹⁰⁶, N.J. Collins¹⁸, C. Collins-Tooth⁵³,
 J. Collot⁵⁵, T. Colombo^{120a,120b}, G. Colon⁸⁵,
 G. Compostella¹⁰⁰, P. Conde Muino^{125a},
 E. Coniavitis¹⁶⁷, M.C. Conidi¹², S.M. Consonni^{90a,90b},

- V. Consorti⁴⁸, S. Constantinescu^{26a}, C. Conta^{120a,120b},
G. Conti⁵⁷, F. Conventi^{103a,i}, M. Cooke¹⁵,
B.D. Cooper⁷⁷, A.M. Cooper-Sarkar¹¹⁹,
N.J. Cooper-Smith⁷⁶, K. Copic¹⁵, T. Cornelissen¹⁷⁶,
M. Corradi^{20a}, F. Corriveau^{86,j}, A. Corso-Radu¹⁶⁴,
A. Cortes-Gonzalez¹⁶⁶, G. Cortiana¹⁰⁰, G. Costa^{90a},
M.J. Costa¹⁶⁸, D. Costanzo¹⁴⁰, D. Côté³⁰, G. Cottin^{32a},
L. Courneyea¹⁷⁰, G. Cowan⁷⁶, B.E. Cox⁸³,
K. Cranmer¹⁰⁹, S. Crépe-Renaudin⁵⁵, F. Crescioli⁷⁹,
M. Cristinziani²¹, G. Crosetti^{37a,37b}, C.-M. Cuciuc^{26a},
C. Cuenca Almenar¹⁷⁷, T. Cuhadar Donszelmann¹⁴⁰,
J. Cummings¹⁷⁷, M. Curatolo⁴⁷, C.J. Curtis¹⁸,
C. Cuthbert¹⁵¹, H. Czirr¹⁴², P. Czodrowski⁴⁴,
Z. Czyczula¹⁷⁷, S. D'Auria⁵³, M. D'Onofrio⁷³,
A. D'Orazio^{133a,133b},
M.J. Da Cunha Sargedas De Sousa^{125a}, C. Da Via⁸³,
W. Dabrowski^{38a}, A. Dafinca¹¹⁹, T. Dai⁸⁸,
F. Dallaire⁹⁴, C. Dallapiccola⁸⁵, M. Dam³⁶,
D.S. Damiani¹³⁸, A.C. Daniells¹⁸, H.O. Danielsson³⁰,
V. Dao¹⁰⁵, G. Darbo^{50a}, G.L. Darlea^{26c}, S. Darmora⁸,
J.A. Dassoulas⁴², W. Davey²¹, T. Davidek¹²⁸,
N. Davidson⁸⁷, E. Davies^{119,d}, M. Davies⁹⁴,
O. Davignon⁷⁹, A.R. Davison⁷⁷, Y. Davygora^{58a},
E. Dawe¹⁴³, I. Dawson¹⁴⁰,
R.K. Daya-Ishmukhametova²³, K. De⁸,
R. de Asmundis^{103a}, S. De Castro^{20a,20b}, S. De Cecco⁷⁹,
J. de Graat⁹⁹, N. De Groot¹⁰⁵, P. de Jong¹⁰⁶,
C. De La Taille¹¹⁶, H. De la Torre⁸¹, F. De Lorenzi⁶³,
L. De Nooij¹⁰⁶, D. De Pedis^{133a}, A. De Salvo^{133a},
U. De Sanctis^{165a,165c}, A. De Santo¹⁵⁰,
J.B. De Vivie De Regie¹¹⁶, G. De Zorzi^{133a,133b},
W.J. Dearnaley⁷¹, R. Debbe²⁵, C. Debenedetti⁴⁶,
B. Dechenaux⁵⁵, D.V. Dedovich⁶⁴, J. Degenhardt¹²¹,
J. Del Peso⁸¹, T. Del Prete^{123a,123b}, T. Delemontex⁵⁵,
M. Deliyergiyev⁷⁴, A. Dell'Acqua³⁰, L. Dell'Asta²²,
M. Della Pietra^{103a,i}, D. della Volpe^{103a,103b},
M. Delmastro⁵, P.A. Delsart⁵⁵, C. Deluca¹⁰⁶,
S. Demers¹⁷⁷, M. Demichev⁶⁴, A. Demilly⁷⁹,
B. Demirkoz^{12,k}, S.P. Denisov¹²⁹, D. Derendarz³⁹,
J.E. Derkaoui^{136d}, F. Derue⁷⁹, P. Dervan⁷³, K. Desch²¹,
P.O. Deviveiros¹⁰⁶, A. Dewhurst¹³⁰, B. DeWilde¹⁴⁹,
S. Dhaliwal¹⁰⁶, R. Dhullipudi^{78,l}, A. Di Ciaccio^{134a,134b},
L. Di Ciaccio⁵, C. Di Donato^{103a,103b}, A. Di Girolamo³⁰,
B. Di Girolamo³⁰, S. Di Luise^{135a,135b}, A. Di Mattia¹⁵³,
B. Di Micco^{135a,135b}, R. Di Nardo⁴⁷,
A. Di Simone^{134a,134b}, R. Di Sipio^{20a,20b}, M.A. Diaz^{32a},
E.B. Diehl⁸⁸, J. Dietrich⁴², T.A. Dietzsch^{58a},
S. Diglio⁸⁷, K. Dindar Yagci⁴⁰, J. Dingfelder²¹,
F. Dinut^{26a}, C. Dionisi^{133a,133b}, P. Dita^{26a}, S. Dita^{26a},
F. Dittus³⁰, F. Djama⁸⁴, T. Djobava^{51b},
M.A.B. do Vale^{24c}, A. Do Valle Wemans^{125a,m},
T.K.O. Doan⁵, D. Dobos³⁰, E. Dobson⁷⁷, J. Dodd³⁵,
C. Dogliani⁴⁹, T. Doherty⁵³, T. Dohmae¹⁵⁶, Y. Doi^{65,*},
J. Dolejsi¹²⁸, Z. Dolezal¹²⁸, B.A. Dolgoshein^{97,*},
M. Donadelli^{24d}, J. Donini³⁴, J. Dopke³⁰, A. Doria^{103a},
A. Dos Anjos¹⁷⁴, A. Dotti^{123a,123b}, M.T. Dova⁷⁰,
A.T. Doyle⁵³, M. Dris¹⁰, J. Dubbert⁸⁸, S. Dube¹⁵,
E. Dubreuil³⁴, E. Duchovni¹⁷³, G. Duckeck⁹⁹,
D. Duda¹⁷⁶, A. Dudarev³⁰, F. Dudziak⁶³, L. Dufflot¹¹⁶,
M-A. Dufour⁸⁶, L. Duguid⁷⁶, M. Dührssen³⁰,
M. Dunford^{58a}, H. Duran Yildiz^{4a}, M. Düren⁵²,
M. Dwuznik^{38a}, J. Ebke⁹⁹, S. Eckweiler⁸², W. Edson²,
C.A. Edwards⁷⁶, N.C. Edwards⁵³, W. Ehrenfeld²¹,
T. Eifert¹⁴⁴, G. Eigen¹⁴, K. Einsweiler¹⁵,
E. Eisenhandler⁷⁵, T. Ekelo¹⁶⁷, M. El Kacimi^{136c},
M. Ellert¹⁶⁷, S. Elles⁵, F. Ellinghaus⁸², K. Ellis⁷⁵,
N. Ellis³⁰, J. Elmsheuser⁹⁹, M. Elsing³⁰,
D. Emelianov¹³⁰, Y. Enari¹⁵⁶, O.C. Endner⁸²,
R. Engelmann¹⁴⁹, A. Engl⁹⁹, J. Erdmann¹⁷⁷,
A. Ereditato¹⁷, D. Eriksson^{147a}, J. Ernst², M. Ernst²⁵,
J. Ernwein¹³⁷, D. Errede¹⁶⁶, S. Errede¹⁶⁶, E. Ertel⁸²,
M. Escalier¹¹⁶, H. Esch⁴³, C. Escobar¹²⁴,
X. Espinal Curull¹², B. Esposito⁴⁷, F. Etienne⁸⁴,
A.I. Etievre¹³⁷, E. Etzion¹⁵⁴, D. Evangelakou⁵⁴,
H. Evans⁶⁰, L. Fabbri^{20a,20b}, C. Fabre³⁰, G. Facini³⁰,
R.M. Fakhruddinov¹²⁹, S. Falciano^{133a}, Y. Fang^{33a},
M. Fanti^{90a,90b}, A. Farbin⁸, A. Farilla^{135a},
T. Farooque¹⁵⁹, S. Farrell¹⁶⁴, S.M. Farrington¹⁷¹,
P. Farthouat³⁰, F. Fassi¹⁶⁸, P. Fassnacht³⁰,
D. Fassouliotis⁹, B. Fatholahzadeh¹⁵⁹,
A. Favareto^{90a,90b}, L. Fayard¹¹⁶, P. Federic^{145a},
O.L. Fedin¹²², W. Fedorko¹⁶⁹, M. Fehling-Kaschek⁴⁸,
L. Felgioni⁸⁴, C. Feng^{33d}, E.J. Feng⁶, H. Feng⁸⁸,
A.B. Fenyuk¹²⁹, J. Ferencei^{145b}, W. Fernando⁶,
S. Ferrag⁵³, J. Ferrando⁵³, V. Ferrara⁴², A. Ferrari¹⁶⁷,
P. Ferrari¹⁰⁶, R. Ferrari^{120a}, D.E. Ferreira de Lima⁵³,
A. Ferrer¹⁶⁸, D. Ferrere⁴⁹, C. Ferretti⁸⁸,
A. Ferretto Parodi^{50a,50b}, M. Fiassarini³¹, F. Fiedler⁸²,
A. Filipčić⁷⁴, F. Filthaut¹⁰⁵, M. Fincke-Keeler¹⁷⁰,
K.D. Finelli⁴⁵, M.C.N. Fiolhais^{125a,h}, L. Fiorini¹⁶⁸,
A. Firan⁴⁰, J. Fischer¹⁷⁶, M.J. Fisher¹¹⁰,
E.A. Fitzgerald²³, M. Flechl⁴⁸, I. Fleck¹⁴²,
P. Fleischmann¹⁷⁵, S. Fleischmann¹⁷⁶, G.T. Fletcher¹⁴⁰,
G. Fletcher⁷⁵, T. Flick¹⁷⁶, A. Floderus⁸⁰,
L.R. Flores Castillo¹⁷⁴, A.C. Florez Bustos^{160b},
M.J. Flowerdew¹⁰⁰, T. Fonseca Martin¹⁷,
A. Formica¹³⁷, A. Forti⁸³, D. Fortin^{160a}, D. Fournier¹¹⁶,
H. Fox⁷¹, P. Francavilla¹², M. Franchini^{20a,20b},
S. Franchino³⁰, D. Francis³⁰, M. Franklin⁵⁷, S. Franz³⁰,
M. Fraternali^{120a,120b}, S. Fratina¹²¹, S.T. French²⁸,
C. Friedrich⁴², F. Friedrich⁴⁴, D. Froidevaux³⁰,
J.A. Frost²⁸, C. Fukunaga¹⁵⁷, E. Fullana Torregrosa¹²⁸,
B.G. Fulsom¹⁴⁴, J. Fuster¹⁶⁸, C. Gabaldon³⁰,
O. Gabizon¹⁷³, A. Gabrielli^{20a,20b}, A. Gabrielli^{133a,133b},
S. Gadatsch¹⁰⁶, T. Gadfort²⁵, S. Gadomski⁴⁹,
G. Gagliardi^{50a,50b}, P. Gagnon⁶⁰, C. Galea⁹⁹,
B. Galhardo^{125a}, E.J. Gallas¹¹⁹, V. Gallo¹⁷,
B.J. Gallop¹³⁰, P. Gallus¹²⁷, K.K. Gan¹¹⁰,
R.P. Gandrajula⁶², Y.S. Gao^{144,f}, A. Gaponenko¹⁵,
F.M. Garay Walls⁴⁶, F. Garberson¹⁷⁷, C. Garcia¹⁶⁸,
J.E. Garcia Navarro¹⁶⁸, M. Garcia-Sciveres¹⁵,
R.W. Gardner³¹, N. Garelli¹⁴⁴, V. Garonne³⁰,
C. Gatti⁴⁷, G. Gaudio^{120a}, B. Gaur¹⁴², L. Gauthier⁹⁴,
P. Gauzzi^{133a,133b}, I.L. Gavrilenko⁹⁵, C. Gay¹⁶⁹,
G. Gaycken²¹, E.N. Gazis¹⁰, P. Ge^{33d,n}, Z. Gece¹⁶⁹,
C.N.P. Gee¹³⁰, D.A.A. Geerts¹⁰⁶, Ch. Geich-Gimbel²¹,

- K. Gellerstedt^{147a,147b}, C. Gemme^{50a}, A. Gemmell⁵³, M.H. Genest⁵⁵, S. Gentile^{133a,133b}, M. George⁵⁴, S. George⁷⁶, D. Gerbaudo¹⁶⁴, A. Gershon¹⁵⁴, H. Ghazlane^{136b}, N. Ghodbane³⁴, B. Giacobbe^{20a}, S. Giagu^{133a,133b}, V. Giangiobbe¹², P. Giannetti^{123a,123b}, F. Gianotti³⁰, B. Gibbard²⁵, A. Gibson¹⁵⁹, S.M. Gibson³⁰, M. Gilchriese¹⁵, T.P.S. Gillam²⁸, D. Gillberg³⁰, A.R. Gillman¹³⁰, D.M. Gingrich^{3,e}, N. Giokaris⁹, M.P. Giordani^{165c}, R. Giordano^{103a,103b}, F.M. Giorgi¹⁶, P. Giovannini¹⁰⁰, P.F. Giraud¹³⁷, D. Giugni^{90a}, C. Giuliani⁴⁸, M. Giunta⁹⁴, B.K. Gjelsten¹¹⁸, I. Gkialas^{155,o}, L.K. Gladilin⁹⁸, C. Glasman⁸¹, J. Glatzer²¹, A. Glazov⁴², G.L. Glonti⁶⁴, J.R. Goddard⁷⁵, J. Godfrey¹⁴³, J. Godlewski³⁰, M. Goebel⁴², C. Goeringer⁸², S. Goldfarb⁸⁸, T. Golling¹⁷⁷, D. Golubkov¹²⁹, A. Gomes^{125a,c}, L.S. Gomez Fajardo⁴², R. Gonçalo⁷⁶, J. Goncalves Pinto Firmino Da Costa⁴², L. Gonella²¹, S. González de la Hoz¹⁶⁸, G. Gonzalez Parra¹², M.L. Gonzalez Silva²⁷, S. Gonzalez-Sevilla⁴⁹, J.J. Goodson¹⁴⁹, L. Goossens³⁰, P.A. Gorbounov⁹⁶, H.A. Gordon²⁵, I. Gorelov¹⁰⁴, G. Gorfine¹⁷⁶, B. Gorini³⁰, E. Gorini^{72a,72b}, A. Gorišek⁷⁴, E. Gornicki³⁹, A.T. Goshaw⁶, C. Gössling⁴³, M.I. Gostkin⁶⁴, I. Gough Eschrich¹⁶⁴, M. Gouighri^{136a}, D. Goujdami^{136c}, M.P. Goulette⁴⁹, A.G. Goussiou¹³⁹, C. Goy⁵, S. Gozpinar²³, L. Graber⁵⁴, I. Grabowska-Bold^{38a}, P. Grafström^{20a,20b}, K-J. Grahn⁴², E. Gramstad¹¹⁸, F. Grancagnolo^{72a}, S. Grancagnolo¹⁶, V. Grassi¹⁴⁹, V. Gratchev¹²², H.M. Gray³⁰, J.A. Gray¹⁴⁹, E. Graziani^{135a}, O.G. Grebenyuk¹²², T. Greenshaw⁷³, Z.D. Greenwood^{78,l}, K. Gregersen³⁶, I.M. Gregor⁴², P. Grenier¹⁴⁴, J. Griffiths⁸, N. Grigalashvili⁶⁴, A.A. Grillo¹³⁸, K. Grimm⁷¹, S. Grinstein¹², Ph. Gris³⁴, Y.V. Grishkevich⁹⁸, J.-F. Grivaz¹¹⁶, J.P. Grohs⁴⁴, A. Grohsjean⁴², E. Gross¹⁷³, J. Grosse-Knetter⁵⁴, J. Groth-Jensen¹⁷³, K. Grybel¹⁴², F. Guescini⁴⁹, D. Guest¹⁷⁷, O. Gueta¹⁵⁴, C. Guicheney³⁴, E. Guido^{50a,50b}, T. Guillemin¹¹⁶, S. Guindon², U. Gul⁵³, J. Gunther¹²⁷, J. Guo³⁵, P. Gutierrez¹¹², N. Guttman¹⁵⁴, O. Gutzwiller¹⁷⁴, C. Guyot¹³⁷, C. Gwenlan¹¹⁹, C.B. Gwilliam⁷³, A. Haas¹⁰⁹, S. Haas³⁰, C. Haber¹⁵, H.K. Hadavand⁸, P. Haefner²¹, Z. Hajduk³⁹, H. Hakobyan¹⁷⁸, D. Hall¹¹⁹, G. Halladjian⁶², K. Hamacher¹⁷⁶, P. Hamal¹¹⁴, K. Hamano⁸⁷, M. Hamer⁵⁴, A. Hamilton^{146a,p}, S. Hamilton¹⁶², L. Han^{33b}, K. Hanagaki¹¹⁷, K. Hanawa¹⁶¹, M. Hance¹⁵, C. Handel⁸², P. Hanke^{58a}, J.R. Hansen³⁶, J.B. Hansen³⁶, J.D. Hansen³⁶, P.H. Hansen³⁶, P. Hansson¹⁴⁴, K. Hara¹⁶¹, A.S. Hard¹⁷⁴, T. Harenberg¹⁷⁶, S. Harkusha⁹¹, D. Harper⁸⁸, R.D. Harrington⁴⁶, O.M. Harris¹³⁹, J. Hartert⁴⁸, F. Hartjes¹⁰⁶, T. Haruyama⁶⁵, A. Harvey⁵⁶, S. Hasegawa¹⁰², Y. Hasegawa¹⁴¹, S. Hassani¹³⁷, S. Haug¹⁷, M. Hauschild³⁰, R. Hauser⁸⁹, M. Havranek²¹, C.M. Hawkes¹⁸, R.J. Hawkings³⁰, A.D. Hawkins⁸⁰, T. Hayakawa⁶⁶, T. Hayashi¹⁶¹, D. Hayden⁷⁶, C.P. Hays¹¹⁹, H.S. Hayward⁷³, S.J. Haywood¹³⁰, S.J. Head¹⁸, T. Heck⁸², V. Hedberg⁸⁰, L. Heelan⁸, S. Heim¹²¹, B. Heinemann¹⁵, S. Heisterkamp³⁶, J. Hejbal¹²⁶, L. Helary²², C. Heller⁹⁹, M. Heller³⁰, S. Hellman^{147a,147b}, D. Hellmich²¹, C. Helsen³⁰, J. Henderson¹¹⁹, R.C.W. Henderson⁷¹, M. Henke^{58a}, A. Henrichs¹⁷⁷, A.M. Henriques Correia³⁰, S. Henrot-Versille¹¹⁶, C. Hensel⁵⁴, G.H. Herbert¹⁶, C.M. Hernandez⁸, Y. Hernández Jiménez¹⁶⁸, R. Herrberg-Schubert¹⁶, G. Herten⁴⁸, R. Hertenberger⁹⁹, L. Hervas³⁰, G.G. Hesketh⁷⁷, N.P. Hesse¹⁰⁶, R. Hickling⁷⁵, E. Higón-Rodríguez¹⁶⁸, J.C. Hill²⁸, K.H. Hiller⁴², S. Hillert²¹, S.J. Hillier¹⁸, I. Hinchliffe¹⁵, E. Hines¹²¹, M. Hirose¹¹⁷, D. Hirschbuehl¹⁷⁶, J. Hobbs¹⁴⁹, N. Hod¹⁰⁶, M.C. Hodgkinson¹⁴⁰, P. Hodgson¹⁴⁰, A. Hoecker³⁰, M.R. Hoferkamp¹⁰⁴, J. Hoffman⁴⁰, D. Hoffmann⁸⁴, J.I. Hofmann^{58a}, M. Hohlfeld⁸², S.O. Holmgren^{147a}, J.L. Holzbauer⁸⁹, T.M. Hong¹²¹, L. Hooft van Huysduynen¹⁰⁹, J.-Y. Hostachy⁵⁵, S. Hou¹⁵², A. Hoummada^{136a}, J. Howard¹¹⁹, J. Howarth⁸³, M. Hrabovsky¹¹⁴, I. Hristova¹⁶, J. Hrivnac¹¹⁶, T. Hryn'ova⁵, P.J. Hsu⁸², S.-C. Hsu¹³⁹, D. Hu³⁵, X. Hu²⁵, Z. Hubacek³⁰, F. Hubaut⁸⁴, F. Huegging²¹, A. Huettmann⁴², T.B. Huffman¹¹⁹, E.W. Hughes³⁵, G. Hughes⁷¹, M. Huhtinen³⁰, T.A. Hülsing⁸², M. Hurwitz¹⁵, N. Huseynov^{64,q}, J. Huston⁸⁹, J. Huth⁵⁷, G. Iacobucci⁴⁹, G. Iakovidis¹⁰, I. Ibragimov¹⁴², L. Iconomidou-Fayard¹¹⁶, J. Idarraga¹¹⁶, P. Iengo^{103a}, O. Igonkina¹⁰⁶, Y. Ikegami⁶⁵, K. Ikematsu¹⁴², M. Ikeno⁶⁵, D. Iliadis¹⁵⁵, N. Ilic¹⁵⁹, T. Ince¹⁰⁰, P. Ioannou⁹, M. Iodice^{135a}, K. Iordanidou⁹, V. Ippolito^{133a,133b}, A. Irlés Quiles¹⁶⁸, C. Isaksson¹⁶⁷, M. Ishino⁶⁷, M. Ishitsuka¹⁵⁸, R. Ishmukhametov¹¹⁰, C. Issever¹¹⁹, S. Istin^{19a}, A.V. Ivashin¹²⁹, W. Iwanski³⁹, H. Iwasaki⁶⁵, J.M. Izen⁴¹, V. Izzo^{103a}, B. Jackson¹²¹, J.N. Jackson⁷³, P. Jackson¹, M.R. Jaekel³⁰, V. Jain², K. Jakobs⁴⁸, S. Jakobsen³⁶, T. Jakoubek¹²⁶, J. Jakubek¹²⁷, D.O. Jamin¹⁵², D.K. Jana¹¹², E. Jansen⁷⁷, H. Jansen³⁰, J. Janssen²¹, A. Jantsch¹⁰⁰, M. Janus⁴⁸, R.C. Jared¹⁷⁴, G. Jarlskog⁸⁰, L. Jeanty⁵⁷, G.-Y. Jeng¹⁵¹, I. Jen-La Plante³¹, D. Jennens⁸⁷, P. Jenni³⁰, J. Jentzsch⁴³, C. Jeske¹⁷¹, P. Jež³⁶, S. Jézéquel⁵, M.K. Jha^{20a}, H. Ji¹⁷⁴, W. Ji⁸², J. Jia¹⁴⁹, Y. Jiang^{33b}, M. Jimenez Belenguer⁴², S. Jin^{33a}, O. Jinnouchi¹⁵⁸, M.D. Joergensen³⁶, D. Joffe⁴⁰, M. Johansen^{147a,147b}, K.E. Johansson^{147a}, P. Johansson¹⁴⁰, S. Johnert⁴², K.A. Johns⁷, K. Jon-And^{147a,147b}, G. Jones¹⁷¹, R.W.L. Jones⁷¹, T.J. Jones⁷³, P.M. Jorge^{125a}, K.D. Joshi⁸³, J. Jovicevic¹⁴⁸, T. Jovin^{13b}, X. Ju¹⁷⁴, C.A. Jung⁴³, R.M. Jungst³⁰, P. Jussel⁶¹, A. Juste Rozas¹², S. Kabana¹⁷, M. Kaci¹⁶⁸, A. Kaczmarska³⁹, P. Kadlecik³⁶, M. Kado¹¹⁶, H. Kagan¹¹⁰, M. Kagan⁵⁷, E. Kajomovitz¹⁵³, S. Kalinin¹⁷⁶, S. Kama⁴⁰, N. Kanaya¹⁵⁶, M. Kaneda³⁰, S. Kaneti²⁸, T. Kanno¹⁵⁸, V.A. Kantserov⁹⁷, J. Kanzaki⁶⁵, B. Kaplan¹⁰⁹, A. Kapliy³¹, D. Kar⁵³,

- K. Karakostas¹⁰, M. Karnevskiy⁸², V. Kartvelishvili⁷¹,
A.N. Karyukhin¹²⁹, L. Kashif¹⁷⁴, G. Kasieczka^{58b},
R.D. Kass¹¹⁰, A. Kastanas¹⁴, Y. Kataoka¹⁵⁶,
J. Katzy⁴², V. Kaushik⁷, K. Kawagoe⁶⁹,
T. Kawamoto¹⁵⁶, G. Kawamura⁵⁴, S. Kazama¹⁵⁶,
V.F. Kazanin¹⁰⁸, M.Y. Kazarinov⁶⁴, R. Keeler¹⁷⁰,
P.T. Keener¹²¹, R. Kehoe⁴⁰, M. Keil⁵⁴, J.S. Keller¹³⁹,
H. Keoshkerian⁵, O. Kepka¹²⁶, B.P. Kerševan⁷⁴,
S. Kersten¹⁷⁶, K. Kessoku¹⁵⁶, J. Keung¹⁵⁹,
F. Khalil-zada¹¹, H. Khandanyan^{147a,147b},
A. Khanov¹¹³, D. Kharchenko⁶⁴, A. Khodinov⁹⁷,
A. Khomich^{58a}, T.J. Khoo²⁸, G. Khoriali²¹,
A. Khoroshilov¹⁷⁶, V. Khovanskiy⁹⁶, E. Khramov⁶⁴,
J. Khubua^{51b}, H. Kim^{147a,147b}, S.H. Kim¹⁶¹,
N. Kimura¹⁷², O. Kind¹⁶, B.T. King⁷³, M. King⁶⁶,
R.S.B. King¹¹⁹, S.B. King¹⁶⁹, J. Kirk¹³⁰,
A.E. Kiryunin¹⁰⁰, T. Kishimoto⁶⁶, D. Kisielewska^{38a},
T. Kitamura⁶⁶, T. Kittelmann¹²⁴, K. Kiuchi¹⁶¹,
E. Kladiva^{145b}, M. Klein⁷³, U. Klein⁷³,
K. Kleinknecht⁸², M. Klemetti⁸⁶, A. Klier¹⁷³,
P. Klimek^{147a,147b}, A. Klimentov²⁵, R. Klingenberg⁴³,
J.A. Klinger⁸³, E.B. Klinkby³⁶, T. Klioutchnikova³⁰,
P.F. Klok¹⁰⁵, E.-E. Kluge^{58a}, P. Kluit¹⁰⁶, S. Kluth¹⁰⁰,
E. Kneringer⁶¹, E.B.F.G. Knoops⁸⁴, A. Knue⁵⁴,
B.R. Ko⁴⁵, T. Kobayashi¹⁵⁶, M. Kobel⁴⁴, M. Kocian¹⁴⁴,
P. Kodys¹²⁸, S. Koenig⁸², F. Koetsveld¹⁰⁵,
P. Koevesarki²¹, T. Koffas²⁹, E. Koffeman¹⁰⁶,
L.A. Kogan¹¹⁹, S. Kohlmann¹⁷⁶, F. Kohn⁵⁴,
Z. Kohout¹²⁷, T. Kohriki⁶⁵, T. Koi¹⁴⁴, H. Kolanoski¹⁶,
I. Koletsou^{90a}, J. Koll⁸⁹, A.A. Komar⁹⁵, Y. Komori¹⁵⁶,
T. Kondo⁶⁵, K. Köneke³⁰, A.C. König¹⁰⁵, T. Kono^{42,r},
A.I. Kononov⁴⁸, R. Konoplich^{109,s}, N. Konstantinidis⁷⁷,
R. Kopeliansky¹⁵³, S. Koperny^{38a}, L. Köpke⁸²,
A.K. Kopp⁴⁸, K. Korcyl³⁹, K. Kordas¹⁵⁵, A. Korn⁴⁶,
A. Korol¹⁰⁸, I. Korolkov¹², E.V. Korolkova¹⁴⁰,
V.A. Korotkov¹²⁹, O. Kortner¹⁰⁰, S. Kortner¹⁰⁰,
V.V. Kostyukhin²¹, S. Kotov¹⁰⁰, V.M. Kotov⁶⁴,
A. Kotwal⁴⁵, C. Kourkoumelis⁹, V. Kouskoura¹⁵⁵,
A. Koutsman^{160a}, R. Kowalewski¹⁷⁰, T.Z. Kowalski^{38a},
W. Kozanecki¹³⁷, A.S. Kozhin¹²⁹, V. Kral¹²⁷,
V.A. Kramarenko⁹⁸, G. Kramberger⁷⁴, M.W. Krasny⁷⁹,
A. Krasznahorkay¹⁰⁹, J.K. Kraus²¹, A. Kravchenko²⁵,
S. Kreiss¹⁰⁹, J. Kretzschmar⁷³, K. Kreutzfeldt⁵²,
N. Krieger⁵⁴, P. Krieger¹⁵⁹, K. Kroeninger⁵⁴,
H. Kroha¹⁰⁰, J. Kroll¹²¹, J. Kroseberg²¹, J. Krstic^{13a},
U. Kruchonak⁶⁴, H. Krüger²¹, T. Kruker¹⁷,
N. Krumnack⁶³, Z.V. Krumshteyn⁶⁴, A. Kruse¹⁷⁴,
M.K. Kruse⁴⁵, T. Kubota⁸⁷, S. Kudah^{4a}, S. Kuehn⁴⁸,
A. Kugel^{58c}, T. Kuhl⁴², V. Kukhtin⁶⁴, Y. Kulchitsky⁹¹,
S. Kuleshov^{32b}, M. Kuna⁷⁹, J. Kunkle¹²¹, A. Kupco¹²⁶,
H. Kurashige⁶⁶, M. Kurata¹⁶¹, Y.A. Kurochkin⁹¹,
V. Kus¹²⁶, E.S. Kuwertz¹⁴⁸, M. Kuze¹⁵⁸, J. Kvita¹⁴³,
R. Kwee¹⁶, A. La Rosa⁴⁹, L. La Rotonda^{37a,37b},
L. Labarga⁸¹, S. Lablak^{136a}, C. Lacasta¹⁶⁸,
F. Lacava^{133a,133b}, J. Lacey²⁹, H. Lacker¹⁶,
D. Lacour⁷⁹, V.R. Lacuesta¹⁶⁸, E. Ladygin⁶⁴,
R. Lafaye⁵, B. Laforge⁷⁹, T. Lagouri¹⁷⁷, S. Lai⁴⁸,
H. Laier^{58a}, E. Laisne⁵⁵, L. Lambourne⁷⁷,
C.L. Lampen⁷, W. Lampl⁷, E. Lançon¹³⁷,
U. Landgraf⁴⁸, M.P.J. Landon⁷⁵, V.S. Lang^{58a},
C. Lange⁴², A.J. Lankford¹⁶⁴, F. Lanni²⁵,
K. Lantzsos³⁰, A. Lanza^{120a}, S. Laplace⁷⁹, C. Lapoire²¹,
J.F. Laporte¹³⁷, T. Lari^{90a}, A. Larner¹¹⁹, M. Lassnig³⁰,
P. Laurelli⁴⁷, V. Lavorini^{37a,37b}, W. Lavrijsen¹⁵,
P. Laycock⁷³, O. Le Dortz⁷⁹, E. Le Guirriec⁸⁴,
E. Le Menedeu¹², T. LeCompte⁶, F. Ledroit-Guillon⁵⁵,
H. Lee¹⁰⁶, J.S.H. Lee¹¹⁷, S.C. Lee¹⁵², L. Lee¹⁷⁷,
G. Lefebvre⁷⁹, M. Lefebvre¹⁷⁰, M. Legendre¹³⁷,
F. Legger⁹⁹, C. Leggett¹⁵, A. Lehan⁷³, M. Lehmacher²¹,
G. Lehmann Miotto³⁰, A.G. Leister¹⁷⁷, M.A.L. Leite^{24d},
R. Leitner¹²⁸, D. Lellouch¹⁷³, B. Lemmer⁵⁴,
V. Lendermann^{58a}, K.J.C. Leney^{146c}, T. Lenz¹⁰⁶,
G. Lenzen¹⁷⁶, B. Lenzi³⁰, K. Leonhardt⁴⁴,
S. Leontsinis¹⁰, F. Lepold^{58a}, C. Leroy⁹⁴,
J.-R. Lessard¹⁷⁰, C.G. Lester²⁸, C.M. Lester¹²¹,
J. Levêque⁵, D. Levin⁸⁸, L.J. Levinson¹⁷³, A. Lewis¹¹⁹,
G.H. Lewis¹⁰⁹, A.M. Leyko²¹, M. Leyton¹⁶, B. Li^{33b},
B. Li⁸⁴, H. Li¹⁴⁹, H.L. Li³¹, S. Li^{33b,t}, X. Li⁸⁸,
Z. Liang^{119,u}, H. Liao³⁴, B. Liberti^{134a}, P. Lichard³⁰,
K. Lie¹⁶⁶, J. Liebal²¹, W. Liebig¹⁴, C. Limbach²¹,
A. Limosani⁸⁷, M. Limper⁶², S.C. Lin^{152,v}, F. Linde¹⁰⁶,
B.E. Lindquist¹⁴⁹, J.T. Linnemann⁸⁹, E. Lipeles¹²¹,
A. Lipniacka¹⁴, M. Lisovsky⁴², T.M. Liss¹⁶⁶,
D. Lissauer²⁵, A. Lister¹⁶⁹, A.M. Litke¹³⁸, D. Liu¹⁵²,
J.B. Liu^{33b}, K. Liu^{33b,w}, L. Liu⁸⁸, M. Liu⁴⁵, M. Liu^{33b},
Y. Liu^{33b}, M. Livan^{120a,120b}, S.S.A. Livermore¹¹⁹,
A. Lleres⁵⁵, J. Llorente Merino⁸¹, S.L. Lloyd⁷⁵,
F. Lo Sterzo^{133a,133b}, E. Lobodzinska⁴², P. Loch⁷,
W.S. Lockman¹³⁸, T. Loddenkoetter²¹,
F.K. Loebinger⁸³, A.E. Loevschall-Jensen³⁶,
A. Loginov¹⁷⁷, C.W. Loh¹⁶⁹, T. Lohse¹⁶,
K. Lohwasser⁴⁸, M. Lokajicek¹²⁶, V.P. Lombardo⁵,
R.E. Long⁷¹, L. Lopes^{125a}, D. Lopez Mateos⁵⁷,
J. Lorenz⁹⁹, N. Lorenzo Martinez¹¹⁶, M. Losada¹⁶³,
P. Loscutoff¹⁵, M.J. Losty^{160a,*}, X. Lou⁴¹, A. Lounis¹¹⁶,
K.F. Loureiro¹⁶³, J. Love⁶, P.A. Love⁷¹, A.J. Lowe^{144,f},
F. Lu^{33a}, H.J. Lubatti¹³⁹, C. Luci^{133a,133b},
A. Lucotte⁵⁵, D. Ludwig⁴², I. Ludwig⁴⁸, J. Ludwig⁴⁸,
F. Luehring⁶⁰, W. Lukas⁶¹, L. Luminari^{133a},
E. Lund¹¹⁸, J. Lundberg^{147a,147b}, O. Lundberg^{147a,147b},
B. Lund-Jensen¹⁴⁸, J. Lundquist³⁶, M. Lungwitz⁸²,
D. Lynn²⁵, R. Lysak¹²⁶, E. Lytken⁸⁰, H. Ma²⁵,
L.L. Ma¹⁷⁴, G. Maccarrone⁴⁷, A. Macchiolo¹⁰⁰,
B. Maček⁷⁴, J. Machado Miguens^{125a}, D. Macina³⁰,
R. Mackeprang³⁶, R. Madar⁴⁸, R.J. Madaras¹⁵,
H.J. Maddocks⁷¹, W.F. Mader⁴⁴, A. Madsen¹⁶⁷,
M. Maeno⁵, T. Maeno²⁵, L. Magnoni¹⁶⁴,
E. Magradze⁵⁴, K. Mahboubi⁴⁸, J. Mahlstedt¹⁰⁶,
S. Mahmoud⁷³, G. Mahout¹⁸, C. Maiani¹³⁷,
C. Maidantchik^{24a}, A. Maio^{125a,c}, S. Majewski¹¹⁵,
Y. Makida⁶⁵, N. Makovec¹¹⁶, P. Mal^{137,x},
B. Malaescu⁷⁹, Pa. Malecki³⁹, P. Malecki³⁹,
V.P. Maleev¹²², F. Malek⁵⁵, U. Mallik⁶², D. Malon⁶,
C. Malone¹⁴⁴, S. Maltezos¹⁰, V. Malyshev¹⁰⁸,
S. Malyukov³⁰, J. Mamuzic^{13b}, L. Mandelli^{90a},
I. Mandić⁷⁴, R. Mandrysch⁶², J. Maneira^{125a},

- A. Manfredini¹⁰⁰, L. Manhaes de Andrade Filho^{24b},
 J.A. Manjarres Ramos¹³⁷, A. Mann⁹⁹,
 P.M. Manning¹³⁸, A. Manousakis-Katsikakis⁹,
 B. Mansoulie¹³⁷, R. Mantifel⁸⁶, L. Mapelli³⁰,
 L. March¹⁶⁸, J.F. Marchand²⁹, F. Marchese^{134a,134b},
 G. Marchiori⁷⁹, M. Marcisovskiy¹²⁶, C.P. Marino¹⁷⁰,
 C.N. Marques^{125a}, F. Marroquin^{24a}, Z. Marshall¹²¹,
 L.F. Marti¹⁷, S. Marti-Garcia¹⁶⁸, B. Martin³⁰,
 B. Martin⁸⁹, J.P. Martin⁹⁴, T.A. Martin¹⁷¹,
 V.J. Martin⁴⁶, B. Martin dit Latour⁴⁹, H. Martinez¹³⁷,
 M. Martinez¹², S. Martin-Haugh¹⁵⁰, A.C. Martyniuk¹⁷⁰,
 M. Marx⁸³, F. Marzano^{133a}, A. Marzin¹¹², L. Masetti⁸²,
 T. Mashimo¹⁵⁶, R. Mashinistov⁹⁵, J. Masik⁸³,
 A.L. Maslennikov¹⁰⁸, I. Massa^{20a,20b}, N. Massol⁵,
 P. Mastrandrea¹⁴⁹, A. Mastroberardino^{37a,37b},
 T. Masubuchi¹⁵⁶, H. Matsunaga¹⁵⁶, T. Matsushita⁶⁶,
 P. Mättig¹⁷⁶, S. Mättig⁴², C. Mattravers^{119,d},
 J. Maurer⁸⁴, S.J. Maxfield⁷³, D.A. Maximov^{108,g},
 R. Mazini¹⁵², M. Mazur²¹, L. Mazzaferro^{134a,134b},
 M. Mazzanti^{90a}, S.P. Mc Kee⁸⁸, A. McCarn¹⁶⁶,
 R.L. McCarthy¹⁴⁹, T.G. McCarthy²⁹,
 N.A. McCubbin¹³⁰, K.W. McFarlane^{56,*},
 J.A. Mcfayden¹⁴⁰, G. Mchedlidze^{51b}, T. McLaughlan¹⁸,
 S.J. McMahon¹³⁰, R.A. McPherson^{170,j}, A. Meade⁸⁵,
 J. Mechnich¹⁰⁶, M. Mechtel¹⁷⁶, M. Medinnis⁴²,
 S. Meehan³¹, R. Meera-Lebbai¹¹², T. Meguro¹¹⁷,
 S. Mehlhase³⁶, A. Mehta⁷³, K. Meier^{58a}, C. Meineck⁹⁹,
 B. Meirose⁸⁰, C. Melachrinou³¹,
 B.R. Mellado Garcia^{146c}, F. Meloni^{90a,90b},
 L. Mendoza Navas¹⁶³, A. Mengarelli^{20a,20b},
 S. Menke¹⁰⁰, E. Meoni¹⁶², K.M. Mercurio⁵⁷,
 N. Meric¹³⁷, P. Mermoud⁴⁹, L. Merola^{103a,103b},
 C. Meroni^{90a}, F.S. Merritt³¹, H. Merritt¹¹⁰,
 A. Messina^{30,y}, J. Metcalfe²⁵, A.S. Mete¹⁶⁴,
 C. Meyer⁸², C. Meyer³¹, J-P. Meyer¹³⁷, J. Meyer³⁰,
 J. Meyer⁵⁴, S. Michal³⁰, R.P. Middleton¹³⁰, S. Migas⁷³,
 L. Mijovic¹³⁷, G. Mikenberg¹⁷³, M. Mikestikova¹²⁶,
 M. Mikuz⁷⁴, D.W. Miller³¹, W.J. Mills¹⁶⁹, C. Mills⁵⁷,
 A. Milov¹⁷³, D.A. Milstead^{147a,147b}, D. Milstein¹⁷³,
 A.A. Minaenko¹²⁹, M. Miñano Moya¹⁶⁸,
 I.A. Minashvili⁶⁴, A.I. Mincer¹⁰⁹, B. Mindur^{38a},
 M. Mineev⁶⁴, Y. Ming¹⁷⁴, L.M. Mir¹², G. Mirabelli^{133a},
 J. Mitrevski¹³⁸, V.A. Mitsou¹⁶⁸, S. Mitsui⁶⁵,
 P.S. Miyagawa¹⁴⁰, J.U. Mjörnmark⁸⁰, T. Moa^{147a,147b},
 V. Moeller²⁸, S. Mohapatra¹⁴⁹, W. Mohr⁴⁸,
 R. Moles-Valls¹⁶⁸, A. Molfetas³⁰, K. Mönig⁴²,
 C. Monini⁵⁵, J. Monk³⁶, E. Monnier⁸⁴,
 J. Montejo Berlingen¹², F. Monticelli⁷⁰,
 S. Monzani^{20a,20b}, R.W. Moore³, C. Mora Herrera⁴⁹,
 A. Moraes⁵³, N. Morange⁶², J. Morel⁵⁴, D. Moreno⁸²,
 M. Moreno Llácer¹⁶⁸, P. Morettini^{50a},
 M. Morgenstern⁴⁴, M. Morii⁵⁷, S. Moritz⁸²,
 A.K. Morley³⁰, G. Mornacchi³⁰, J.D. Morris⁷⁵,
 L. Morvaj¹⁰², N. Möser²¹, H.G. Moser¹⁰⁰,
 M. Mosidze^{51b}, J. Moss¹¹⁰, R. Mount¹⁴⁴,
 E. Mountricha^{10,z}, S.V. Mouraviev^{95,*},
 E.J.W. Moyse⁸⁵, R.D. Mudd¹⁸, F. Mueller^{58a},
 J. Mueller¹²⁴, K. Mueller²¹, T. Mueller²⁸, T. Mueller⁸²,
 D. Muenstermann³⁰, Y. Munwes¹⁵⁴,
 J.A. Murillo Quijada¹⁸, W.J. Murray¹³⁰, I. Mussche¹⁰⁶,
 E. Musto¹⁵³, A.G. Myagkov^{129,aa}, M. Myska¹²⁶,
 O. Nackenhorst⁵⁴, J. Nadal¹², K. Nagai¹⁶¹, R. Nagai¹⁵⁸,
 Y. Nagai⁸⁴, K. Nagano⁶⁵, A. Nagarkar¹¹⁰,
 Y. Nagasaka⁵⁹, M. Nagel¹⁰⁰, A.M. Nairz³⁰,
 Y. Nakahama³⁰, K. Nakamura⁶⁵, T. Nakamura¹⁵⁶,
 I. Nakano¹¹¹, H. Namasivayam⁴¹, G. Nanava²¹,
 A. Napier¹⁶², R. Narayan^{58b}, M. Nash^{77,d},
 T. Nattermann²¹, T. Naumann⁴², G. Navarro¹⁶³,
 H.A. Neal⁸⁸, P.Yu. Nechaeva⁹⁵, T.J. Neep⁸³,
 A. Negri^{120a,120b}, G. Negri³⁰, M. Negrini^{20a},
 S. Nektarijevic⁴⁹, A. Nelson¹⁶⁴, T.K. Nelson¹⁴⁴,
 S. Nemecek¹²⁶, P. Nemethy¹⁰⁹, A.A. Nepomuceno^{24a},
 M. Nessi^{30,ab}, M.S. Neubauer¹⁶⁶, M. Neumann¹⁷⁶,
 A. Neusiedl⁸², R.M. Neves¹⁰⁹, P. Nevski²⁵,
 F.M. Newcomer¹²¹, P.R. Newman¹⁸, D.H. Nguyen⁶,
 V. Nguyen Thi Hong¹³⁷, R.B. Nickerson¹¹⁹,
 R. Nicolaidou¹³⁷, B. Nicquevert³⁰, F. Niedercorn¹¹⁶,
 J. Nielsen¹³⁸, N. Nikiforou³⁵, A. Nikiforov¹⁶,
 V. Nikolaenko^{129,aa}, I. Nikolic-Audit⁷⁹, K. Nikolics⁴⁹,
 K. Nikolopoulos¹⁸, P. Nilsson⁸, Y. Ninomiya¹⁵⁶,
 A. Nisati^{133a}, R. Nisius¹⁰⁰, T. Nobe¹⁵⁸, L. Nodulman⁶,
 M. Nomachi¹¹⁷, I. Nomidis¹⁵⁵, S. Norberg¹¹²,
 M. Nordberg³⁰, J. Novakova¹²⁸, M. Nozaki⁶⁵,
 L. Nozka¹¹⁴, A.-E. Nuncio-Quiroz²¹,
 G. Nunes Hamninger⁸⁷, T. Nunnemann⁹⁹, E. Nurse⁷⁷,
 B.J. O'Brien⁴⁶, D.C. O'Neil¹⁴³, V. O'Shea⁵³,
 L.B. Oakes⁹⁹, F.G. Oakham^{29,e}, H. Oberlack¹⁰⁰,
 J. Ocariz⁷⁹, A. Ochi⁶⁶, M.I. Ochoa⁷⁷, S. Oda⁶⁹,
 S. Odaka⁶⁵, J. Odier⁸⁴, H. Ogren⁶⁰, A. Oh⁸³, S.H. Oh⁴⁵,
 C.C. Ohm³⁰, T. Ohshima¹⁰², W. Okamura¹¹⁷,
 H. Okawa²⁵, Y. Okumura³¹, T. Okuyama¹⁵⁶,
 A. Olariu^{26a}, A.G. Olchevski⁶⁴, S.A. Olivares Pino⁴⁶,
 M. Oliveira^{125a,h}, D. Oliveira Damazio²⁵,
 E. Oliver Garcia¹⁶⁸, D. Olivito¹²¹, A. Olszewski³⁹,
 J. Olszowska³⁹, A. Onofre^{125a,ac}, P.U.E. Onyisi^{31,ad},
 C.J. Oram^{160a}, M.J. Oreglia³¹, Y. Oren¹⁵⁴,
 D. Orestano^{135a,135b}, N. Orlando^{72a,72b},
 C. Oropeza Barrera⁵³, R.S. Orr¹⁵⁹, B. Osculati^{50a,50b},
 R. Ospanov¹²¹, G. Otero y Garzon²⁷,
 J.P. Ottersbach¹⁰⁶, M. Ouchrif^{136d}, E.A. Ouellette¹⁷⁰,
 F. Ould-Saada¹¹⁸, A. Ouraou¹³⁷, Q. Ouyang^{33a},
 A. Ovcharova¹⁵, M. Owen⁸³, S. Owen¹⁴⁰,
 V.E. Ozcan^{19a}, N. Ozturk⁸, A. Pacheco Pages¹²,
 C. Padilla Aranda¹², S. Pagan Griso¹⁵, E. Paganis¹⁴⁰,
 C. Pahl¹⁰⁰, F. Paige²⁵, P. Pais⁸⁵, K. Pajchel¹¹⁸,
 G. Palacino^{160b}, C.P. Paleari⁷, S. Palestini³⁰,
 D. Pallin³⁴, A. Palma^{125a}, J.D. Palmer¹⁸, Y.B. Pan¹⁷⁴,
 E. Panagiotopoulou¹⁰, J.G. Panduro Vazquez⁷⁶,
 P. Pani¹⁰⁶, N. Panikashvili⁸⁸, S. Panitkin²⁵,
 D. Pantea^{26a}, A. Papadelis^{147a}, Th.D. Papadopoulou¹⁰,
 K. Papageorgiou^{155,o}, A. Paramonov⁶,
 D. Paredes Hernandez³⁴, W. Park^{25,ae}, M.A. Parker²⁸,
 F. Parodi^{50a,50b}, J.A. Parsons³⁵, U. Parzefall⁴⁸,
 S. Pashapour⁵⁴, E. Pasqualucci^{133a}, S. Passaggio^{50a},
 A. Passeri^{135a}, F. Pastore^{135a,135b,*}, Fr. Pastore⁷⁶,
 G. Pásztor^{49,af}, S. Pataria¹⁷⁶, N.D. Patel¹⁵¹,

- J.R. Pater⁸³, S. Patricelli^{103a,103b}, T. Pauly³⁰,
 J. Pearce¹⁷⁰, M. Pedersen¹¹⁸, S. Pedraza Lopez¹⁶⁸,
 M.I. Pedraza Morales¹⁷⁴, S.V. Peleganchuk¹⁰⁸,
 D. Pelikan¹⁶⁷, H. Peng^{33b}, B. Penning³¹, A. Penson³⁵,
 J. Penwell⁶⁰, T. Perez Cavalcanti⁴²,
 E. Perez Codina^{160a}, M.T. Pérez García-Estañ¹⁶⁸,
 V. Perez Reale³⁵, L. Perini^{90a,90b}, H. Pernegger³⁰,
 R. Perrino^{72a}, P. Perrodo⁵, V.D. Peshekhonov⁶⁴,
 K. Peters³⁰, R.F.Y. Peters^{54,ag}, B.A. Petersen³⁰,
 J. Petersen³⁰, T.C. Petersen³⁶, E. Petit⁵,
 A. Petridis^{147a,147b}, C. Petridou¹⁵⁵, E. Petrolo^{133a},
 F. Petrucci^{135a,135b}, D. Petschull⁴², M. Petteni¹⁴³,
 R. Pezoa^{32b}, A. Phan⁸⁷, P.W. Phillips¹³⁰,
 G. Piacquadio¹⁴⁴, E. Pianori¹⁷¹, A. Picazio⁴⁹,
 E. Piccaro⁷⁵, M. Piccinini^{20a,20b}, S.M. Piec⁴²,
 R. Piegai²⁷, D.T. Pignotti¹¹⁰, J.E. Pilcher³¹,
 A.D. Pilkington⁷⁷, J. Pina^{125a,c},
 M. Pinamonti^{165a,165c,ah}, A. Pinder¹¹⁹, J.L. Pinfeld³,
 A. Pingel³⁶, B. Pinto^{125a}, C. Pizio^{90a,90b},
 M.-A. Pleier²⁵, V. Pleskot¹²⁸, E. Plotnikova⁶⁴,
 P. Plucinski^{147a,147b}, A. Poblaguev²⁵, S. Poddar^{58a},
 F. Podlaski³⁴, R. Poettgen⁸², L. Poggioli¹¹⁶, D. Pohl²¹,
 M. Pohl⁴⁹, G. Polesello^{120a}, A. Policicchio^{37a,37b},
 R. Polifka¹⁵⁹, A. Polini^{20a}, V. Polychronakos²⁵,
 D. Pomeroy²³, K. Pommès³⁰, L. Pontecorvo^{133a},
 B.G. Pope⁸⁹, G.A. Popeneciu^{26b}, D.S. Popovic^{13a},
 A. Poppleton³⁰, X. Portell Bueso¹², G.E. Pospelov¹⁰⁰,
 S. Pospisil¹²⁷, I.N. Potrap⁶⁴, C.J. Potter¹⁵⁰,
 C.T. Potter¹¹⁵, G. Poulard³⁰, J. Poveda⁶⁰,
 V. Pozdnyakov⁶⁴, R. Prabhu⁷⁷, P. Pralavorio⁸⁴,
 A. Pranko¹⁵, S. Prasad³⁰, R. Pravahan²⁵, S. Prell⁶³,
 K. Pretzl¹⁷, D. Price⁶⁰, J. Price⁷³, L.E. Price⁶,
 D. Prieur¹²⁴, M. Primavera^{72a}, M. Proissl⁴⁶,
 K. Prokofiev¹⁰⁹, F. Prokoshin^{32b}, E. Protopapadaki¹³⁷,
 S. Protopopescu²⁵, J. Proudfoot⁶, X. Prudent⁴⁴,
 M. Przybycien^{38a}, H. Przysiesniak⁵, S. Psoroulas²¹,
 E. Ptacek¹¹⁵, E. Pueschel⁸⁵, D. Puldon¹⁴⁹,
 M. Purohit^{25,ae}, P. Puzo¹¹⁶, Y. Pylypchenko⁶²,
 J. Qian⁸⁸, A. Quadt⁵⁴, D.R. Quarrie¹⁵, W.B. Quayle¹⁷⁴,
 D. Quilty⁵³, M. Raas¹⁰⁵, V. Radeka²⁵, V. Radescu⁴²,
 P. Radloff¹¹⁵, F. Ragusa^{90a,90b}, G. Rahal¹⁷⁹,
 S. Rajagopalan²⁵, M. Rammensee⁴⁸, M. Rammes¹⁴²,
 A.S. Randle-Conde⁴⁰, K. Randrianarivony²⁹,
 C. Rangel-Smith⁷⁹, K. Rao¹⁶⁴, F. Rauscher⁹⁹,
 T.C. Rave⁴⁸, T. Ravenscroft⁵³, M. Raymond³⁰,
 A.L. Read¹¹⁸, D.M. Rebuzzi^{120a,120b}, A. Redelbach¹⁷⁵,
 G. Redlinger²⁵, R. Reece¹²¹, K. Reeves⁴¹, A. Reinsch¹¹⁵,
 I. Reisinger⁴³, M. Relich¹⁶⁴, C. Rembser³⁰, Z.L. Ren¹⁵²,
 A. Renaud¹¹⁶, M. Rescigno^{133a}, S. Resconi^{90a},
 B. Resende¹³⁷, P. Reznicek⁹⁹, R. Rezvani⁹⁴,
 R. Richter¹⁰⁰, E. Richter-Was^{38b}, M. Ridel⁷⁹,
 P. Rieck¹⁶, M. Rijssenbeek¹⁴⁹, A. Rimoldi^{120a,120b},
 L. Rinaldi^{20a}, R.R. Rios⁴⁰, E. Ritsch⁶¹, I. Riu¹²,
 G. Rivoltella^{90a,90b}, F. Rizatdinova¹¹³, E. Rizvi⁷⁵,
 S.H. Robertson^{86,j}, A. Robichaud-Veronneau¹¹⁹,
 D. Robinson²⁸, J.E.M. Robinson⁸³, A. Robson⁵³,
 J.G. Rocha de Lima¹⁰⁷, C. Roda^{123a,123b},
 D. Roda Dos Santos³⁰, A. Roe⁵⁴, S. Roe³⁰,
 O. Røhne¹¹⁸, S. Rolli¹⁶², A. Romaniouk⁹⁷,
 M. Romano^{20a,20b}, G. Romeo²⁷, E. Romero Adam¹⁶⁸,
 N. Rompotis¹³⁹, L. Roos⁷⁹, E. Ros¹⁶⁸, S. Rosati^{133a},
 K. Rosbach⁴⁹, A. Rose¹⁵⁰, M. Rose⁷⁶,
 G.A. Rosenbaum¹⁵⁹, P.L. Rosendahl¹⁴, O. Rosenthal¹⁴²,
 V. Rossetti¹², E. Rossi^{133a,133b}, L.P. Rossi^{50a},
 M. Rotaru^{26a}, I. Roth¹⁷³, J. Rothberg¹³⁹,
 D. Rousseau¹¹⁶, C.R. Royon¹³⁷, A. Rozanov⁸⁴,
 Y. Rozen¹⁵³, X. Ruan^{33a,ai}, F. Rubbo¹², I. Rubinskiy⁴²,
 N. Ruckstuhl¹⁰⁶, V.I. Rud⁹⁸, C. Rudolph⁴⁴,
 M.S. Rudolph¹⁵⁹, F. Rühr⁷, A. Ruiz-Martinez⁶³,
 L. Rumyantsev⁶⁴, Z. Rurikova⁴⁸, N.A. Rusakovich⁶⁴,
 A. Ruschke⁹⁹, J.P. Rutherford⁷, N. Ruthmann⁴⁸,
 P. Ruzicka¹²⁶, Y.F. Ryabov¹²², M. Rybar¹²⁸,
 G. Rybkin¹¹⁶, N.C. Ryder¹¹⁹, A.F. Saavedra¹⁵¹,
 A. Saddique³, I. Sadeh¹⁵⁴, H.F.-W. Sadrozinski¹³⁸,
 R. Sadykov⁶⁴, F. Safai Tehrani^{133a}, H. Sakamoto¹⁵⁶,
 G. Salamanna⁷⁵, A. Salamon^{134a}, M. Saleem¹¹²,
 D. Salek³⁰, D. Salihagic¹⁰⁰, A. Salmikov¹⁴⁴, J. Salt¹⁶⁸,
 B.M. Salvachua Ferrando⁶, D. Salvatore^{37a,37b},
 F. Salvatore¹⁵⁰, A. Salvucci¹⁰⁵, A. Salzburger³⁰,
 D. Sampsonidis¹⁵⁵, A. Sanchez^{103a,103b}, J. Sánchez¹⁶⁸,
 V. Sanchez Martinez¹⁶⁸, H. Sandaker¹⁴, H.G. Sander⁸²,
 M.P. Sanders⁹⁹, M. Sandhoff⁴¹⁷⁶, T. Sandoval²⁸,
 C. Sandoval¹⁶³, R. Sandstroem¹⁰⁰, D.P.C. Sankey¹³⁰,
 A. Sansoni⁴⁷, C. Santoni³⁴, R. Santonico^{134a,134b},
 H. Santos^{125a}, I. Santoyo Castillo¹⁵⁰, K. Sapp¹²⁴,
 J.G. Saraiva^{125a}, T. Sarangi¹⁷⁴,
 E. Sarkisyan-Grinbaum⁸, B. Sarrazin²¹,
 F. Sarri^{123a,123b}, G. Sartisohn¹⁷⁶, O. Sasaki⁶⁵,
 Y. Sasaki¹⁵⁶, N. Sasao⁶⁷, I. Satsounkevitch⁹¹,
 G. Sauvage^{5,*}, E. Sauvan⁵, J.B. Sauvan¹¹⁶,
 P. Savard^{159,e}, V. Savinov¹²⁴, D.O. Savu³⁰,
 C. Sawyer¹¹⁹, L. Sawyer^{78,l}, D.H. Saxon⁵³, J. Saxon¹²¹,
 C. Sbarra^{20a}, A. Sbrizzi³, D.A. Scannicchio¹⁶⁴,
 M. Scarcella¹⁵¹, J. Schaarschmidt¹¹⁶, P. Schacht¹⁰⁰,
 D. Schaefer¹²¹, A. Schaelicke⁴⁶, S. Schaepe²¹,
 S. Schaezel^{58b}, U. Schäfer⁸², A.C. Schaffer¹¹⁶,
 D. Schaile⁹⁹, R.D. Schamberger¹⁴⁹, V. Scharf^{58a},
 V.A. Schegelsky¹²², D. Scheirich⁸⁸, M. Schernau¹⁶⁴,
 M.I. Scherzer³⁵, C. Schiavi^{50a,50b}, J. Schieck⁹⁹,
 C. Schillo⁴⁸, M. Schioppa^{37a,37b}, S. Schlenker³⁰,
 E. Schmidt⁴⁸, K. Schmieden²¹, C. Schmitt⁸²,
 C. Schmitt⁹⁹, S. Schmitt^{58b}, B. Schneider¹⁷,
 Y.J. Schnellbach⁷³, U. Schnoor⁴⁴, L. Schoeffel¹³⁷,
 A. Schoening^{58b}, A.L.S. Schorlemmer⁵⁴, M. Schott⁸²,
 D. Schouten^{160a}, J. Schovancova¹²⁶, M. Schram⁸⁶,
 C. Schroeder⁸², N. Schroer^{58c}, M.J. Schultens²¹,
 H.-C. Schultz-Coulon^{58a}, H. Schulz¹⁶, M. Schumacher⁴⁸,
 B.A. Schumm¹³⁸, Ph. Schune¹³⁷, A. Schwartzman¹⁴⁴,
 Ph. Schwiegler¹⁰⁰, Ph. Schwemling¹³⁷,
 R. Schwinhorst⁸⁹, J. Schwindling¹³⁷, T. Schwindt²¹,
 M. Schwoerer⁵, F.G. Sciacca¹⁷, E. Scifo¹¹⁶, G. Sciolla²³,
 W.G. Scott¹³⁰, F. Scutti²¹, J. Searcy⁸⁸, G. Sedov⁴²,
 E. Sedykh¹²², S.C. Seidel¹⁰⁴, A. Seiden¹³⁸, F. Seifert⁴⁴,
 J.M. Seixas^{24a}, G. Sekhniaidze^{103a}, S.J. Sekula⁴⁰,
 K.E. Selbach⁴⁶, D.M. Seliverstov¹²², G. Sellers⁷³,
 M. Seman^{145b}, N. Semprini-Cesari^{20a,20b}, C. Serfon³⁰,

- L. Serin¹¹⁶, L. Serkin⁵⁴, T. Serre⁸⁴, R. Seuster^{160a},
H. Severini¹¹², A. Sfyrla³⁰, E. Shabalina⁵⁴,
M. Shamim¹¹⁵, L.Y. Shan^{33a}, J.T. Shank²²,
Q.T. Shao⁸⁷, M. Shapiro¹⁵, P.B. Shatalov⁹⁶,
K. Shaw^{165a,165c}, P. Sherwood⁷⁷, S. Shimizu¹⁰²,
M. Shimojima¹⁰¹, T. Shin⁵⁶, M. Shiyakova⁶⁴,
A. Shmeleva⁹⁵, M.J. Shochet³¹, D. Short¹¹⁹,
S. Shrestha⁶³, E. Shulga⁹⁷, M.A. Shupe⁷, P. Sicho¹²⁶,
A. Sidoti^{133a}, F. Siegert⁴⁸, Dj. Sijacki^{13a}, O. Silbert¹⁷³,
J. Silva^{125a}, Y. Silver¹⁵⁴, D. Silverstein¹⁴⁴,
S.B. Silverstein^{147a}, V. Simak¹²⁷, O. Simard⁵,
Lj. Simic^{13a}, S. Simion¹¹⁶, E. Simioni⁸², B. Simmons⁷⁷,
R. Simoniello^{90a,90b}, M. Simonyan³⁶, P. Sinervo¹⁵⁹,
N.B. Sinev¹¹⁵, V. Sipica¹⁴², G. Siragusa¹⁷⁵, A. Sircar⁷⁸,
A.N. Sisakyan^{64,*}, S.Yu. Sivoklokov⁹⁸, J. Sjölin^{147a,147b},
T.B. Sjursen¹⁴, L.A. Skinnari¹⁵, H.P. Skottowe⁵⁷,
K. Skovpen¹⁰⁸, P. Skubic¹¹², M. Slater¹⁸, T. Slavicek¹²⁷,
K. Sliwa¹⁶², V. Smakhtin¹⁷³, B.H. Smart⁴⁶,
L. Smestad¹¹⁸, S.Yu. Smirnov⁹⁷, Y. Smirnov⁹⁷,
L.N. Smirnova^{98,aj}, O. Smirnova⁸⁰, K.M. Smith⁵³,
M. Smizanska⁷¹, K. Smolek¹²⁷, A.A. Snesarev⁹⁵,
G. Snidero⁷⁵, J. Snow¹¹², S. Snyder²⁵, R. Sobie^{170,j},
J. Sodomka¹²⁷, A. Soffer¹⁵⁴, D.A. Soh^{152,u},
C.A. Solans³⁰, M. Solar¹²⁷, J. Solc¹²⁷, E.Yu. Soldatov⁹⁷,
U. Soldevila¹⁶⁸, E. Solfaroli Camillocci^{133a,133b},
A.A. Solodkov¹²⁹, O.V. Solovyanov¹²⁹, V. Solovyev¹²²,
N. Soni¹, A. Sood¹⁵, V. Sopko¹²⁷, B. Sopko¹²⁷,
M. Sosebee⁸, R. Soualah^{165a,165c}, P. Soueid⁹⁴,
A. Soukharev¹⁰⁸, D. South⁴², S. Spagnolo^{72a,72b},
F. Spano⁷⁶, R. Spighi^{20a}, G. Spigo³⁰, R. Spiwojs³⁰,
M. Spousta^{128,ak}, T. Spreitzer¹⁵⁹, B. Spurlock⁸,
R.D. St. Denis⁵³, J. Stahlman¹²¹, R. Stamen^{58a},
E. Stanecka³⁹, R.W. Stanek⁶, C. Stanescu^{135a},
M. Stanescu-Bellu⁴², M.M. Stanitzki⁴², S. Stapnes¹¹⁸,
E.A. Starchenko¹²⁹, J. Stark⁵⁵, P. Staroba¹²⁶,
P. Starovoitov⁴², R. Staszewski³⁹, A. Staude⁹⁹,
P. Stavina^{145a,*}, G. Steele⁵³, P. Steinbach⁴⁴,
P. Steinberg²⁵, I. Stekl¹²⁷, B. Stelzer¹⁴³, H.J. Stelzer⁸⁹,
O. Stelzer-Chilton^{160a}, H. Stenzel⁵², S. Stern¹⁰⁰,
G.A. Stewart³⁰, J.A. Stillings²¹, M.C. Stockton⁸⁶,
M. Stoebe⁸⁶, K. Stoerig⁴⁸, G. Stoicea^{26a}, S. Stonjek¹⁰⁰,
A.R. Stradling⁸, A. Straessner⁴⁴, J. Strandberg¹⁴⁸,
S. Strandberg^{147a,147b}, A. Strandlie¹¹⁸, M. Strang¹¹⁰,
E. Strauss¹⁴⁴, M. Strauss¹¹², P. Strizenc^{145b},
R. Ströhmer¹⁷⁵, D.M. Strom¹¹⁵, J.A. Strong^{76,*},
R. Stroynowski⁴⁰, B. Stugu¹⁴, I. Stumer^{25,*},
J. Stupak¹⁴⁹, P. Sturm¹⁷⁶, N.A. Styles⁴², D. Su¹⁴⁴,
H.S. Subramania³, R. Subramaniam⁷⁸, A. Succurro¹²,
Y. Sugaya¹¹⁷, C. Suhr¹⁰⁷, M. Suk¹²⁷, V.V. Sulin⁹⁵,
S. Sultansoy^{4c}, T. Sumida⁶⁷, X. Sun⁵⁵,
J.E. Sundermann⁴⁸, K. Suruliz¹⁴⁰, G. Susinno^{37a,37b},
M.R. Sutton¹⁵⁰, Y. Suzuki⁶⁵, Y. Suzuki⁶⁶, M. Svatos¹²⁶,
S. Swedish¹⁶⁹, M. Swiatlowski¹⁴⁴, I. Sykora^{145a},
T. Sykora¹²⁸, D. Ta¹⁰⁶, K. Tackmann⁴², A. Taffard¹⁶⁴,
R. Tafirout^{160a}, N. Taiblum¹⁵⁴, Y. Takahashi¹⁰²,
H. Takai²⁵, R. Takashima⁶⁸, H. Takeda⁶⁶,
T. Takeshita¹⁴¹, Y. Takubo⁶⁵, M. Talby⁸⁴,
A. Talyshev^{108,g}, J.Y.C. Tam¹⁷⁵, M.C. Tamsett^{78,al},
K.G. Tan⁸⁷, J. Tanaka¹⁵⁶, R. Tanaka¹¹⁶, S. Tanaka¹³²,
S. Tanaka⁶⁵, A.J. Tanasijczuk¹⁴³, K. Tani⁶⁶,
N. Tannoury⁸⁴, S. Tapprogge⁸², S. Tarem¹⁵³,
F. Tarrade²⁹, G.F. Tartarelli^{90a}, P. Tas¹²⁸,
M. Tasevsky¹²⁶, T. Tashiro⁶⁷, E. Tassi^{37a,37b},
Y. Tayalati^{136d}, C. Taylor⁷⁷, F.E. Taylor⁹³,
G.N. Taylor⁸⁷, W. Taylor^{160b}, M. Teinturier¹¹⁶,
F.A. Teischinger³⁰, M. Teixeira Dias Castanheira⁷⁵,
P. Teixeira-Dias⁷⁶, K.K. Temming⁴⁸, H. Ten Kate³⁰,
P.K. Teng¹⁵², S. Terada⁶⁵, K. Terashi¹⁵⁶, J. Terron⁸¹,
M. Testa⁴⁷, R.J. Teuscher^{159,j}, J. Therhaag²¹,
T. Theveneaux-Pelzer³⁴, S. Thoma⁴⁸, J.P. Thomas¹⁸,
E.N. Thompson³⁵, P.D. Thompson¹⁸,
P.D. Thompson¹⁵⁹, A.S. Thompson⁵³, L.A. Thomsen³⁶,
E. Thomson¹²¹, M. Thomson²⁸, W.M. Thong⁸⁷,
R.P. Thun^{88,*}, F. Tian³⁵, M.J. Tibbetts¹⁵, T. Tic¹²⁶,
V.O. Tikhomirov⁹⁵, Y.A. Tikhonov^{108,g},
S. Timoshenko⁹⁷, E. Tiouchichine⁸⁴, P. Tipton¹⁷⁷,
S. Tisserant⁸⁴, T. Todorov⁵, S. Todorova-Nova¹⁶²,
B. Toggerson¹⁶⁴, J. Tojo⁶⁹, S. Tokár^{145a},
K. Tokushuku⁶⁵, K. Tollefson⁸⁹, L. Tomlinson⁸³,
M. Tomoto¹⁰², L. Tompkins³¹, K. Toms¹⁰⁴,
A. Tonoyan¹⁴, C. Topfel¹⁷, N.D. Topilin⁶⁴,
E. Torrence¹¹⁵, H. Torres⁷⁹, E. Torró Pastor¹⁶⁸,
J. Toth^{84,af}, F. Touchard⁸⁴, D.R. Tovey¹⁴⁰,
H.L. Tran¹¹⁶, T. Trefzger¹⁷⁵, L. Tremblet³⁰,
A. Tricoli³⁰, I.M. Trigger^{160a}, S. Trincaz-Duvoid⁷⁹,
M.F. Tripiana⁷⁰, N. Triplett²⁵, W. Trischuk¹⁵⁹,
B. Trocme⁵⁵, C. Troncon^{90a}, M. Trottier-McDonald¹⁴³,
M. Trovatelli^{135a,135b}, P. True⁸⁹, M. Trzebinski³⁹,
A. Trzupek³⁹, C. Tsarouchas³⁰, J.C.-L. Tseng¹¹⁹,
M. Tsiakiris¹⁰⁶, P.V. Tsiarshka⁹¹, D. TSIONOU¹³⁷,
G. Tsipolitis¹⁰, S. Tsiskaridze¹², V. Tsiskaridze⁴⁸,
E.G. Tskhadadze^{51a}, I.I. Tsukerman⁹⁶, V. Tsulaia¹⁵,
J.-W. Tsung²¹, S. Tsuno⁶⁵, D. Tsybychev¹⁴⁹, A. Tua¹⁴⁰,
A. Tudorache^{26a}, V. Tudorache^{26a}, J.M. Tuggle³¹,
A.N. Tuna¹²¹, M. Turala³⁹, D. Turecek¹²⁷,
I. Turk Cakir^{4d}, R. Turra^{90a,90b}, P.M. Tuts³⁵,
A. Tykhonov⁷⁴, M. Tylmad^{147a,147b}, M. Tyndel¹³⁰,
K. Uchida²¹, I. Ueda¹⁵⁶, R. Ueno²⁹, M. Ughetto⁸⁴,
M. Ugland¹⁴, M. Uhlenbrock²¹, F. Ukegawa¹⁶¹,
G. Unal³⁰, A. Undrus²⁵, G. Unel¹⁶⁴, F.C. Ungaro⁴⁸,
Y. Unno⁶⁵, D. Urbaniec³⁵, P. Urquijo²¹, G. Usai⁸,
L. Vacavant⁸⁴, V. Vacek¹²⁷, B. Vachon⁸⁶, S. Vahsen¹⁵,
N. Valencic¹⁰⁶, S. Valentinetti^{20a,20b}, A. Valero¹⁶⁸,
L. Valery³⁴, S. Valkar¹²⁸, E. Valladolid Gallego¹⁶⁸,
S. Vallecorsa¹⁵³, J.A. Valls Ferrer¹⁶⁸, R. Van Berg¹²¹,
P.C. Van Der Deijl¹⁰⁶, R. van der Geer¹⁰⁶,
H. van der Graaf¹⁰⁶, R. Van Der Leeuw¹⁰⁶,
D. van der Ster³⁰, N. van Eldik³⁰, P. van Gemmeren⁶,
J. Van Nieuwkoop¹⁴³, I. van Vulpen¹⁰⁶, M. Vanadia¹⁰⁰,
W. Vandelli³⁰, A. Vaniachine⁶, P. Vankov⁴²,
F. Vannucci⁷⁹, R. Vari^{133a}, E.W. Varnes⁷, T. Varol⁸⁵,
D. Varouchas¹⁵, A. Vartapetian⁸, K.E. Varvell¹⁵¹,
V.I. Vassilakopoulos⁵⁶, F. Vazeille³⁴,
T. Vazquez Schroeder⁵⁴, F. Veloso^{125a}, S. Veneziano^{133a},
A. Ventura^{72a,72b}, D. Ventura⁸⁵, M. Venturi⁴⁸,
N. Venturi¹⁵⁹, V. Vercesi^{120a}, M. Verducci¹³⁹,

- W. Verkerke¹⁰⁶, J.C. Vermeulen¹⁰⁶, A. Vest⁴⁴,
M.C. Vetterli^{143,e}, I. Vichou¹⁶⁶, T. Vickey^{146c,am},
O.E. Vickey Boeriu^{146c}, G.H.A. Viehhauser¹¹⁹,
S. Viel¹⁶⁹, M. Villa^{20a,20b}, M. Villaplana Perez¹⁶⁸,
E. Vilucchi⁴⁷, M.G. Vincter²⁹, V.B. Vinogradov⁶⁴,
J. Virzi¹⁵, O. Vitells¹⁷³, M. Viti⁴², I. Vivarelli⁴⁸,
F. Vives Vaque³, S. Vlachos¹⁰, D. Vladoiu⁹⁹,
M. Vlasak¹²⁷, A. Vogel²¹, P. Vokac¹²⁷, G. Volpi⁴⁷,
M. Volpi⁸⁷, G. Volpini^{90a}, H. von der Schmitt¹⁰⁰,
H. von Radziewski⁴⁸, E. von Toerne²¹, V. Vorobel¹²⁸,
M. Vos¹⁶⁸, R. Voss³⁰, J.H. Vosseveld⁷³, N. Vranjes¹³⁷,
M. Vranjes Milosavljevic¹⁰⁶, V. Vrba¹²⁶,
M. Vreeswijk¹⁰⁶, T. Vu Anh⁴⁸, R. Vuillermet³⁰,
I. Vukotic³¹, Z. Vykydal¹²⁷, W. Wagner¹⁷⁶,
P. Wagner²¹, S. Wahrmund⁴⁴, J. Wakabayashi¹⁰²,
S. Walch⁸⁸, J. Walder⁷¹, R. Walker⁹⁹,
W. Walkowiak¹⁴², R. Wall¹⁷⁷, P. Waller⁷³, B. Walsh¹⁷⁷,
C. Wang⁴⁵, H. Wang¹⁷⁴, H. Wang⁴⁰, J. Wang¹⁵²,
J. Wang^{33a}, K. Wang⁸⁶, R. Wang¹⁰⁴, S.M. Wang¹⁵²,
T. Wang²¹, X. Wang¹⁷⁷, A. Warburton⁸⁶, C.P. Ward²⁸,
D.R. Wardrope⁷⁷, M. Warsinsky⁴⁸, A. Washbrook⁴⁶,
C. Wasicki⁴², I. Watanabe⁶⁶, P.M. Watkins¹⁸,
A.T. Watson¹⁸, I.J. Watson¹⁵¹, M.F. Watson¹⁸,
G. Watts¹³⁹, S. Watts⁸³, A.T. Waugh¹⁵¹,
B.M. Waugh⁷⁷, M.S. Weber¹⁷, J.S. Webster³¹,
A.R. Weidberg¹¹⁹, P. Weigell¹⁰⁰, J. Weingarten⁵⁴,
C. Weiser⁴⁸, P.S. Wells³⁰, T. Wenaus²⁵, D. Wendland¹⁶,
Z. Weng^{152,u}, T. Wengler³⁰, S. Wenig³⁰, N. Wermes²¹,
M. Werner⁴⁸, P. Werner³⁰, M. Werth¹⁶⁴, M. Wessels^{58a},
J. Wetter¹⁶², K. Whalen²⁹, A. White⁸, M.J. White⁸⁷,
R. White^{32b}, S. White^{123a,123b}, S.R. Whitehead¹¹⁹,
D. Whiteson¹⁶⁴, D. Whittington⁶⁰, D. Wicke¹⁷⁶,
F.J. Wickens¹³⁰, W. Wiedenmann¹⁷⁴, M. Wielers^{80,d},
P. Wienemann²¹, C. Wiglesworth³⁶,
L.A.M. Wiik-Fuchs²¹, P.A. Wijeratne⁷⁷,
A. Wildauer¹⁰⁰, M.A. Wildt^{42,r}, I. Wilhelm¹²⁸,
H.G. Wilkens³⁰, J.Z. Will⁹⁹, E. Williams³⁵,
H.H. Williams¹²¹, S. Williams²⁸, W. Willis^{35,*},
S. Willocq⁸⁵, J.A. Wilson¹⁸, A. Wilson⁸⁸,
I. Wingerter-Seez⁵, S. Winkelmann⁴⁸, F. Winklmeier³⁰,
M. Wittgen¹⁴⁴, T. Wittig⁴³, J. Wittkowski⁹⁹,
S.J. Wollstadt⁸², M.W. Wolter³⁹, H. Wolters^{125a,h},
W.C. Wong⁴¹, G. Wooden⁸⁸, B.K. Wosiek³⁹,
J. Wotschack³⁰, M.J. Woudstra⁸³, K.W. Wozniak³⁹,
K. Wraight⁵³, M. Wright⁵³, B. Wrona⁷³, S.L. Wu¹⁷⁴,
X. Wu⁴⁹, Y. Wu⁸⁸, E. Wulf³⁵, B.M. Wynne⁴⁶,
S. Xella³⁶, M. Xiao¹³⁷, S. Xie⁴⁸, C. Xu^{33b,z}, D. Xu^{33a},
L. Xu^{33b}, B. Yabsley¹⁵¹, S. Yacoob^{146b,an},
M. Yamada⁶⁵, H. Yamaguchi¹⁵⁶, Y. Yamaguchi¹⁵⁶,
A. Yamamoto⁶⁵, K. Yamamoto⁶³, S. Yamamoto¹⁵⁶,
T. Yamamura¹⁵⁶, T. Yamazaki¹⁵⁶, K. Yamauchi¹⁰²,
T. Yamazaki¹⁵⁶, Y. Yamazaki⁶⁶, Z. Yan²², H. Yang^{33e},
H. Yang¹⁷⁴, U.K. Yang⁸³, Y. Yang¹¹⁰, Z. Yang^{147a,147b},
S. Yanush⁹², L. Yao^{33a}, Y. Yasu⁶⁵, E. Yatsenko⁴²,
K.H. Yau Wong²¹, J. Ye⁴⁰, S. Ye²⁵, A.L. Yen⁵⁷,
E. Yildirim⁴², M. Yilmaz^{4b}, R. Yoosoofmiya¹²⁴,
K. Yorita¹⁷², R. Yoshida⁶, K. Yoshihara¹⁵⁶,
C. Young¹⁴⁴, C.J.S. Young¹¹⁹, S. Youssef²², D. Yu²⁵,
D.R. Yu¹⁵, J. Yu⁸, J. Yu¹¹³, L. Yuan⁶⁶,
A. Yurkewicz¹⁰⁷, B. Zabinski³⁹, R. Zaidan⁶²,
A.M. Zaitsev^{129,aa}, S. Zambito²³, L. Zanello^{133a,133b},
D. Zanzi¹⁰⁰, A. Zaytsev²⁵, C. Zeitnitz¹⁷⁶, M. Zeman¹²⁷,
A. Zemla³⁹, O. Zenin¹²⁹, T. Ženiš^{145a}, D. Zerwas¹¹⁶,
G. Zevi della Porta⁵⁷, D. Zhang⁸⁸, H. Zhang⁸⁹,
J. Zhang⁶, L. Zhang¹⁵², X. Zhang^{33d}, Z. Zhang¹¹⁶,
Z. Zhao^{33b}, A. Zhemchugov⁶⁴, J. Zhong¹¹⁹, B. Zhou⁸⁸,
N. Zhou¹⁶⁴, Y. Zhou¹⁵², C.G. Zhu^{33d}, H. Zhu⁴²,
J. Zhu⁸⁸, Y. Zhu^{33b}, X. Zhuang^{33a}, A. Zibell⁹⁹,
D. Zieminska⁶⁰, N.I. Zimin⁶⁴, C. Zimmermann⁸²,
R. Zimmermann²¹, S. Zimmermann²¹,
S. Zimmermann⁴⁸, Z. Zinonos^{123a,123b},
M. Ziolkowski¹⁴², R. Zitoun⁵, L. Živković³⁵,
V.V. Zmouchko^{129,*}, G. Zoernig¹⁷⁴, A. Zoccoli^{20a,20b},
M. zur Nedden¹⁶, V. Zutshi¹⁰⁷, L. Zwalinski³⁰.
- ¹ School of Chemistry and Physics, University of
Adelaide, Adelaide, Australia
² Physics Department, SUNY Albany, Albany NY,
United States of America
³ Department of Physics, University of Alberta,
Edmonton AB, Canada
⁴ (a) Department of Physics, Ankara University, Ankara;
(b) Department of Physics, Gazi University, Ankara;
(c) Division of Physics, TOBB University of Economics
and Technology, Ankara; (d) Turkish Atomic Energy
Authority, Ankara, Turkey
⁵ LAPP, CNRS/IN2P3 and Université de Savoie,
Annecy-le-Vieux, France
⁶ High Energy Physics Division, Argonne National
Laboratory, Argonne IL, United States of America
⁷ Department of Physics, University of Arizona, Tucson
AZ, United States of America
⁸ Department of Physics, The University of Texas at
Arlington, Arlington TX, United States of America
⁹ Physics Department, University of Athens, Athens,
Greece
¹⁰ Physics Department, National Technical University
of Athens, Zografou, Greece
¹¹ Institute of Physics, Azerbaijan Academy of Sciences,
Baku, Azerbaijan
¹² Institut de Física d'Altes Energies and Departament
de Física de la Universitat Autònoma de Barcelona and
ICREA, Barcelona, Spain
¹³ (a) Institute of Physics, University of Belgrade,
Belgrade; (b) Vinca Institute of Nuclear Sciences,
University of Belgrade, Belgrade, Serbia
¹⁴ Department for Physics and Technology, University
of Bergen, Bergen, Norway
¹⁵ Physics Division, Lawrence Berkeley National
Laboratory and University of California, Berkeley CA,
United States of America
¹⁶ Department of Physics, Humboldt University, Berlin,
Germany
¹⁷ Albert Einstein Center for Fundamental Physics and
Laboratory for High Energy Physics, University of
Bern, Bern, Switzerland

- ¹⁸ School of Physics and Astronomy, University of Birmingham, Birmingham, United Kingdom
- ¹⁹ ^(a)Department of Physics, Bogazici University, Istanbul; ^(b)Department of Physics, Dogus University, Istanbul; ^(c)Department of Physics Engineering, Gaziantep University, Gaziantep, Turkey
- ²⁰ ^(a)INFN Sezione di Bologna; ^(b)Dipartimento di Fisica, Università di Bologna, Bologna, Italy
- ²¹ Physikalisches Institut, University of Bonn, Bonn, Germany
- ²² Department of Physics, Boston University, Boston MA, United States of America
- ²³ Department of Physics, Brandeis University, Waltham MA, United States of America
- ²⁴ ^(a)Universidade Federal do Rio De Janeiro COPPE/EE/IF, Rio de Janeiro; ^(b)Federal University of Juiz de Fora (UFJF), Juiz de Fora; ^(c)Federal University of Sao Joao del Rei (UFSJ), Sao Joao del Rei; ^(d)Instituto de Fisica, Universidade de Sao Paulo, Sao Paulo, Brazil
- ²⁵ Physics Department, Brookhaven National Laboratory, Upton NY, United States of America
- ²⁶ ^(a)National Institute of Physics and Nuclear Engineering, Bucharest; ^(b)National Institute for Research and Development of Isotopic and Molecular Technologies, Physics Department, Cluj Napoca; ^(c)University Politehnica Bucharest, Bucharest; ^(d)West University in Timisoara, Timisoara, Romania
- ²⁷ Departamento de Física, Universidad de Buenos Aires, Buenos Aires, Argentina
- ²⁸ Cavendish Laboratory, University of Cambridge, Cambridge, United Kingdom
- ²⁹ Department of Physics, Carleton University, Ottawa ON, Canada
- ³⁰ CERN, Geneva, Switzerland
- ³¹ Enrico Fermi Institute, University of Chicago, Chicago IL, United States of America
- ³² ^(a)Departamento de Física, Pontificia Universidad Católica de Chile, Santiago; ^(b)Departamento de Física, Universidad Técnica Federico Santa María, Valparaíso, Chile
- ³³ ^(a)Institute of High Energy Physics, Chinese Academy of Sciences, Beijing; ^(b)Department of Modern Physics, University of Science and Technology of China, Anhui; ^(c)Department of Physics, Nanjing University, Jiangsu; ^(d)School of Physics, Shandong University, Shandong; ^(e)Physics Department, Shanghai Jiao Tong University, Shanghai, China
- ³⁴ Laboratoire de Physique Corpusculaire, Clermont Université and Université Blaise Pascal and CNRS/IN2P3, Clermont-Ferrand, France
- ³⁵ Nevis Laboratory, Columbia University, Irvington NY, United States of America
- ³⁶ Niels Bohr Institute, University of Copenhagen, Kobenhavn, Denmark
- ³⁷ ^(a)INFN Gruppo Collegato di Cosenza; ^(b)Dipartimento di Fisica, Università della Calabria, Rende, Italy
- ³⁸ ^(a)AGH University of Science and Technology, Faculty of Physics and Applied Computer Science, Krakow; ^(b)Marian Smoluchowski Institute of Physics, Jagiellonian University, Krakow, Poland
- ³⁹ The Henryk Niewodniczanski Institute of Nuclear Physics, Polish Academy of Sciences, Krakow, Poland
- ⁴⁰ Physics Department, Southern Methodist University, Dallas TX, United States of America
- ⁴¹ Physics Department, University of Texas at Dallas, Richardson TX, United States of America
- ⁴² DESY, Hamburg and Zeuthen, Germany
- ⁴³ Institut für Experimentelle Physik IV, Technische Universität Dortmund, Dortmund, Germany
- ⁴⁴ Institut für Kern- und Teilchenphysik, Technical University Dresden, Dresden, Germany
- ⁴⁵ Department of Physics, Duke University, Durham NC, United States of America
- ⁴⁶ SUPA - School of Physics and Astronomy, University of Edinburgh, Edinburgh, United Kingdom
- ⁴⁷ INFN Laboratori Nazionali di Frascati, Frascati, Italy
- ⁴⁸ Fakultät für Mathematik und Physik, Albert-Ludwigs-Universität, Freiburg, Germany
- ⁴⁹ Section de Physique, Université de Genève, Geneva, Switzerland
- ⁵⁰ ^(a)INFN Sezione di Genova; ^(b)Dipartimento di Fisica, Università di Genova, Genova, Italy
- ⁵¹ ^(a)E. Andronikashvili Institute of Physics, Iv. Javakhishvili Tbilisi State University, Tbilisi; ^(b)High Energy Physics Institute, Tbilisi State University, Tbilisi, Georgia
- ⁵² II Physikalisches Institut, Justus-Liebig-Universität Giessen, Giessen, Germany
- ⁵³ SUPA - School of Physics and Astronomy, University of Glasgow, Glasgow, United Kingdom
- ⁵⁴ II Physikalisches Institut, Georg-August-Universität, Göttingen, Germany
- ⁵⁵ Laboratoire de Physique Subatomique et de Cosmologie, Université Joseph Fourier and CNRS/IN2P3 and Institut National Polytechnique de Grenoble, Grenoble, France
- ⁵⁶ Department of Physics, Hampton University, Hampton VA, United States of America
- ⁵⁷ Laboratory for Particle Physics and Cosmology, Harvard University, Cambridge MA, United States of America
- ⁵⁸ ^(a)Kirchhoff-Institut für Physik, Ruprecht-Karls-Universität Heidelberg, Heidelberg; ^(b)Physikalisches Institut, Ruprecht-Karls-Universität Heidelberg, Heidelberg; ^(c)ZITI Institut für technische Informatik, Ruprecht-Karls-Universität Heidelberg, Mannheim, Germany
- ⁵⁹ Faculty of Applied Information Science, Hiroshima Institute of Technology, Hiroshima, Japan
- ⁶⁰ Department of Physics, Indiana University, Bloomington IN, United States of America
- ⁶¹ Institut für Astro- und Teilchenphysik, Leopold-Franzens-Universität, Innsbruck, Austria
- ⁶² University of Iowa, Iowa City IA, United States of

America

- ⁶³ Department of Physics and Astronomy, Iowa State University, Ames IA, United States of America
- ⁶⁴ Joint Institute for Nuclear Research, JINR Dubna, Dubna, Russia
- ⁶⁵ KEK, High Energy Accelerator Research Organization, Tsukuba, Japan
- ⁶⁶ Graduate School of Science, Kobe University, Kobe, Japan
- ⁶⁷ Faculty of Science, Kyoto University, Kyoto, Japan
- ⁶⁸ Kyoto University of Education, Kyoto, Japan
- ⁶⁹ Department of Physics, Kyushu University, Fukuoka, Japan
- ⁷⁰ Instituto de Física La Plata, Universidad Nacional de La Plata and CONICET, La Plata, Argentina
- ⁷¹ Physics Department, Lancaster University, Lancaster, United Kingdom
- ⁷² ^(a)INFN Sezione di Lecce; ^(b)Dipartimento di Matematica e Fisica, Università del Salento, Lecce, Italy
- ⁷³ Oliver Lodge Laboratory, University of Liverpool, Liverpool, United Kingdom
- ⁷⁴ Department of Physics, Jožef Stefan Institute and University of Ljubljana, Ljubljana, Slovenia
- ⁷⁵ School of Physics and Astronomy, Queen Mary University of London, London, United Kingdom
- ⁷⁶ Department of Physics, Royal Holloway University of London, Surrey, United Kingdom
- ⁷⁷ Department of Physics and Astronomy, University College London, London, United Kingdom
- ⁷⁸ Louisiana Tech University, Ruston LA, United States of America
- ⁷⁹ Laboratoire de Physique Nucléaire et de Hautes Energies, UPMC and Université Paris-Diderot and CNRS/IN2P3, Paris, France
- ⁸⁰ Fysiska institutionen, Lunds universitet, Lund, Sweden
- ⁸¹ Departamento de Física Teórica C-15, Universidad Autónoma de Madrid, Madrid, Spain
- ⁸² Institut für Physik, Universität Mainz, Mainz, Germany
- ⁸³ School of Physics and Astronomy, University of Manchester, Manchester, United Kingdom
- ⁸⁴ CPPM, Aix-Marseille Université and CNRS/IN2P3, Marseille, France
- ⁸⁵ Department of Physics, University of Massachusetts, Amherst MA, United States of America
- ⁸⁶ Department of Physics, McGill University, Montreal QC, Canada
- ⁸⁷ School of Physics, University of Melbourne, Victoria, Australia
- ⁸⁸ Department of Physics, The University of Michigan, Ann Arbor MI, United States of America
- ⁸⁹ Department of Physics and Astronomy, Michigan State University, East Lansing MI, United States of America
- ⁹⁰ ^(a)INFN Sezione di Milano; ^(b)Dipartimento di Fisica, Università di Milano, Milano, Italy
- ⁹¹ B.I. Stepanov Institute of Physics, National Academy

of Sciences of Belarus, Minsk, Republic of Belarus

- ⁹² National Scientific and Educational Centre for Particle and High Energy Physics, Minsk, Republic of Belarus
- ⁹³ Department of Physics, Massachusetts Institute of Technology, Cambridge MA, United States of America
- ⁹⁴ Group of Particle Physics, University of Montreal, Montreal QC, Canada
- ⁹⁵ P.N. Lebedev Institute of Physics, Academy of Sciences, Moscow, Russia
- ⁹⁶ Institute for Theoretical and Experimental Physics (ITEP), Moscow, Russia
- ⁹⁷ Moscow Engineering and Physics Institute (MEPhI), Moscow, Russia
- ⁹⁸ D.V.Skobel'tsyn Institute of Nuclear Physics, M.V.Lomonosov Moscow State University, Moscow, Russia
- ⁹⁹ Fakultät für Physik, Ludwig-Maximilians-Universität München, München, Germany
- ¹⁰⁰ Max-Planck-Institut für Physik (Werner-Heisenberg-Institut), München, Germany
- ¹⁰¹ Nagasaki Institute of Applied Science, Nagasaki, Japan
- ¹⁰² Graduate School of Science and Kobayashi-Maskawa Institute, Nagoya University, Nagoya, Japan
- ¹⁰³ ^(a)INFN Sezione di Napoli; ^(b)Dipartimento di Scienze Fisiche, Università di Napoli, Napoli, Italy
- ¹⁰⁴ Department of Physics and Astronomy, University of New Mexico, Albuquerque NM, United States of America
- ¹⁰⁵ Institute for Mathematics, Astrophysics and Particle Physics, Radboud University Nijmegen/Nikhef, Nijmegen, Netherlands
- ¹⁰⁶ Nikhef National Institute for Subatomic Physics and University of Amsterdam, Amsterdam, Netherlands
- ¹⁰⁷ Department of Physics, Northern Illinois University, DeKalb IL, United States of America
- ¹⁰⁸ Budker Institute of Nuclear Physics, SB RAS, Novosibirsk, Russia
- ¹⁰⁹ Department of Physics, New York University, New York NY, United States of America
- ¹¹⁰ Ohio State University, Columbus OH, United States of America
- ¹¹¹ Faculty of Science, Okayama University, Okayama, Japan
- ¹¹² Homer L. Dodge Department of Physics and Astronomy, University of Oklahoma, Norman OK, United States of America
- ¹¹³ Department of Physics, Oklahoma State University, Stillwater OK, United States of America
- ¹¹⁴ Palacký University, RCPTM, Olomouc, Czech Republic
- ¹¹⁵ Center for High Energy Physics, University of Oregon, Eugene OR, United States of America
- ¹¹⁶ LAL, Université Paris-Sud and CNRS/IN2P3, Orsay, France
- ¹¹⁷ Graduate School of Science, Osaka University, Osaka, Japan

- ¹¹⁸ Department of Physics, University of Oslo, Oslo, Norway
- ¹¹⁹ Department of Physics, Oxford University, Oxford, United Kingdom
- ¹²⁰ ^(a)INFN Sezione di Pavia; ^(b)Dipartimento di Fisica, Università di Pavia, Pavia, Italy
- ¹²¹ Department of Physics, University of Pennsylvania, Philadelphia PA, United States of America
- ¹²² Petersburg Nuclear Physics Institute, Gatchina, Russia
- ¹²³ ^(a)INFN Sezione di Pisa; ^(b)Dipartimento di Fisica E. Fermi, Università di Pisa, Pisa, Italy
- ¹²⁴ Department of Physics and Astronomy, University of Pittsburgh, Pittsburgh PA, United States of America
- ¹²⁵ ^(a)Laboratorio de Instrumentacao e Fisica Experimental de Particulas - LIP, Lisboa, Portugal; ^(b)Departamento de Fisica Teorica y del Cosmos and CAFPE, Universidad de Granada, Granada, Spain
- ¹²⁶ Institute of Physics, Academy of Sciences of the Czech Republic, Praha, Czech Republic
- ¹²⁷ Czech Technical University in Prague, Praha, Czech Republic
- ¹²⁸ Faculty of Mathematics and Physics, Charles University in Prague, Praha, Czech Republic
- ¹²⁹ State Research Center Institute for High Energy Physics, Protvino, Russia
- ¹³⁰ Particle Physics Department, Rutherford Appleton Laboratory, Didcot, United Kingdom
- ¹³¹ Physics Department, University of Regina, Regina SK, Canada
- ¹³² Ritsumeikan University, Kusatsu, Shiga, Japan
- ¹³³ ^(a)INFN Sezione di Roma I; ^(b)Dipartimento di Fisica, Università La Sapienza, Roma, Italy
- ¹³⁴ ^(a)INFN Sezione di Roma Tor Vergata; ^(b)Dipartimento di Fisica, Università di Roma Tor Vergata, Roma, Italy
- ¹³⁵ ^(a)INFN Sezione di Roma Tre; ^(b)Dipartimento di Matematica e Fisica, Università Roma Tre, Roma, Italy
- ¹³⁶ ^(a)Faculté des Sciences Ain Chock, Réseau Universitaire de Physique des Hautes Energies - Université Hassan II, Casablanca; ^(b)Centre National de l'Énergie des Sciences Techniques Nucleaires, Rabat; ^(c)Faculté des Sciences Semlalia, Université Cadi Ayyad, LPHEA-Marrakech; ^(d)Faculté des Sciences, Université Mohamed Premier and LPTPM, Oujda; ^(e)Faculté des sciences, Université Mohammed V-Agdal, Rabat, Morocco
- ¹³⁷ DSM/IRFU (Institut de Recherches sur les Lois Fondamentales de l'Univers), CEA Saclay (Commissariat à l'Énergie Atomique et aux Énergies Alternatives), Gif-sur-Yvette, France
- ¹³⁸ Santa Cruz Institute for Particle Physics, University of California Santa Cruz, Santa Cruz CA, United States of America
- ¹³⁹ Department of Physics, University of Washington, Seattle WA, United States of America
- ¹⁴⁰ Department of Physics and Astronomy, University of Sheffield, Sheffield, United Kingdom
- ¹⁴¹ Department of Physics, Shinshu University, Nagano, Japan
- ¹⁴² Fachbereich Physik, Universität Siegen, Siegen, Germany
- ¹⁴³ Department of Physics, Simon Fraser University, Burnaby BC, Canada
- ¹⁴⁴ SLAC National Accelerator Laboratory, Stanford CA, United States of America
- ¹⁴⁵ ^(a)Faculty of Mathematics, Physics & Informatics, Comenius University, Bratislava; ^(b)Department of Subnuclear Physics, Institute of Experimental Physics of the Slovak Academy of Sciences, Kosice, Slovak Republic
- ¹⁴⁶ ^(a)Department of Physics, University of Cape Town, Cape Town; ^(b)Department of Physics, University of Johannesburg, Johannesburg; ^(c)School of Physics, University of the Witwatersrand, Johannesburg, South Africa
- ¹⁴⁷ ^(a)Department of Physics, Stockholm University; ^(b)The Oskar Klein Centre, Stockholm, Sweden
- ¹⁴⁸ Physics Department, Royal Institute of Technology, Stockholm, Sweden
- ¹⁴⁹ Departments of Physics & Astronomy and Chemistry, Stony Brook University, Stony Brook NY, United States of America
- ¹⁵⁰ Department of Physics and Astronomy, University of Sussex, Brighton, United Kingdom
- ¹⁵¹ School of Physics, University of Sydney, Sydney, Australia
- ¹⁵² Institute of Physics, Academia Sinica, Taipei, Taiwan
- ¹⁵³ Department of Physics, Technion: Israel Institute of Technology, Haifa, Israel
- ¹⁵⁴ Raymond and Beverly Sackler School of Physics and Astronomy, Tel Aviv University, Tel Aviv, Israel
- ¹⁵⁵ Department of Physics, Aristotle University of Thessaloniki, Thessaloniki, Greece
- ¹⁵⁶ International Center for Elementary Particle Physics and Department of Physics, The University of Tokyo, Tokyo, Japan
- ¹⁵⁷ Graduate School of Science and Technology, Tokyo Metropolitan University, Tokyo, Japan
- ¹⁵⁸ Department of Physics, Tokyo Institute of Technology, Tokyo, Japan
- ¹⁵⁹ Department of Physics, University of Toronto, Toronto ON, Canada
- ¹⁶⁰ ^(a)TRIUMF, Vancouver BC; ^(b)Department of Physics and Astronomy, York University, Toronto ON, Canada
- ¹⁶¹ Faculty of Pure and Applied Sciences, University of Tsukuba, Tsukuba, Japan
- ¹⁶² Department of Physics and Astronomy, Tufts University, Medford MA, United States of America
- ¹⁶³ Centro de Investigaciones, Universidad Antonio Narino, Bogota, Colombia
- ¹⁶⁴ Department of Physics and Astronomy, University of California Irvine, Irvine CA, United States of America
- ¹⁶⁵ ^(a)INFN Gruppo Collegato di Udine; ^(b)ICTP,

Trieste; ^(c) Dipartimento di Chimica, Fisica e Ambiente, Università di Udine, Udine, Italy

¹⁶⁶ Department of Physics, University of Illinois, Urbana IL, United States of America

¹⁶⁷ Department of Physics and Astronomy, University of Uppsala, Uppsala, Sweden

¹⁶⁸ Instituto de Física Corpuscular (IFIC) and Departamento de Física Atómica, Molecular y Nuclear and Departamento de Ingeniería Electrónica and Instituto de Microelectrónica de Barcelona (IMB-CNM), University of Valencia and CSIC, Valencia, Spain

¹⁶⁹ Department of Physics, University of British Columbia, Vancouver BC, Canada

¹⁷⁰ Department of Physics and Astronomy, University of Victoria, Victoria BC, Canada

¹⁷¹ Department of Physics, University of Warwick, Coventry, United Kingdom

¹⁷² Waseda University, Tokyo, Japan

¹⁷³ Department of Particle Physics, The Weizmann Institute of Science, Rehovot, Israel

¹⁷⁴ Department of Physics, University of Wisconsin, Madison WI, United States of America

¹⁷⁵ Fakultät für Physik und Astronomie, Julius-Maximilians-Universität, Würzburg, Germany

¹⁷⁶ Fachbereich C Physik, Bergische Universität Wuppertal, Wuppertal, Germany

¹⁷⁷ Department of Physics, Yale University, New Haven CT, United States of America

¹⁷⁸ Yerevan Physics Institute, Yerevan, Armenia

¹⁷⁹ Centre de Calcul de l'Institut National de Physique Nucléaire et de Physique des Particules (IN2P3), Villeurbanne, France

^a Also at Department of Physics, King's College London, London, United Kingdom

^b Also at Laboratório de Instrumentação e Física Experimental de Partículas - LIP, Lisboa, Portugal

^c Also at Faculdade de Ciências and CFNUL, Universidade de Lisboa, Lisboa, Portugal

^d Also at Particle Physics Department, Rutherford Appleton Laboratory, Didcot, United Kingdom

^e Also at TRIUMF, Vancouver BC, Canada

^f Also at Department of Physics, California State University, Fresno CA, United States of America

^g Also at Novosibirsk State University, Novosibirsk, Russia

^h Also at Department of Physics, University of Coimbra, Coimbra, Portugal

ⁱ Also at Università di Napoli Parthenope, Napoli, Italy

^j Also at Institute of Particle Physics (IPP), Canada

^k Also at Department of Physics, Middle East Technical University, Ankara, Turkey

^l Also at Louisiana Tech University, Ruston LA, United States of America

^m Also at Dep Física and CEFITEC of Faculdade de Ciências e Tecnologia, Universidade Nova de Lisboa, Caparica, Portugal

ⁿ Also at Department of Physics and Astronomy, Michigan State University, East Lansing MI, United States of America

^o Also at Department of Financial and Management Engineering, University of the Aegean, Chios, Greece

^p Also at Department of Physics, University of Cape Town, Cape Town, South Africa

^q Also at Institute of Physics, Azerbaijan Academy of Sciences, Baku, Azerbaijan

^r Also at Institut für Experimentalphysik, Universität Hamburg, Hamburg, Germany

^s Also at Manhattan College, New York NY, United States of America

^t Also at CPPM, Aix-Marseille Université and CNRS/IN2P3, Marseille, France

^u Also at School of Physics and Engineering, Sun Yat-sen University, Guanzhou, China

^v Also at Academia Sinica Grid Computing, Institute of Physics, Academia Sinica, Taipei, Taiwan

^w Also at Laboratoire de Physique Nucléaire et de Hautes Energies, UPMC and Université Paris-Diderot and CNRS/IN2P3, Paris, France

^x Also at School of Physical Sciences, National Institute of Science Education and Research, Bhubaneswar, India

^y Also at Dipartimento di Fisica, Università La Sapienza, Roma, Italy

^z Also at DSM/IRFU (Institut de Recherches sur les Lois Fondamentales de l'Univers), CEA Saclay (Commissariat à l'Energie Atomique et aux Energies Alternatives), Gif-sur-Yvette, France

^{aa} Also at Moscow Institute of Physics and Technology State University, Dolgoprudny, Russia

^{ab} Also at Section de Physique, Université de Genève, Geneva, Switzerland

^{ac} Also at Departamento de Física, Universidade de Minho, Braga, Portugal

^{ad} Also at Department of Physics, The University of Texas at Austin, Austin TX, United States of America

^{ae} Also at Department of Physics and Astronomy, University of South Carolina, Columbia SC, United States of America

^{af} Also at Institute for Particle and Nuclear Physics, Wigner Research Centre for Physics, Budapest, Hungary

^{ag} Also at DESY, Hamburg and Zeuthen, Germany

^{ah} Also at International School for Advanced Studies (SISSA), Trieste, Italy

^{ai} Also at LAL, Université Paris-Sud and CNRS/IN2P3, Orsay, France

^{aj} Also at Faculty of Physics, M.V.Lomonosov Moscow State University, Moscow, Russia

^{ak} Also at Nevis Laboratory, Columbia University, Irvington NY, United States of America

^{al} Also at Physics Department, Brookhaven National Laboratory, Upton NY, United States of America

^{am} Also at Department of Physics, Oxford University, Oxford, United Kingdom

^{an} Also at Discipline of Physics, University of KwaZulu-Natal, Durban, South Africa

* Deceased